Quantum Gravity Beyond the End of the World

Zixia Wei

Yukawa Institute for Theoretical Physics
Kyoto University

Abstract

The holographic principle has played a crucial role in studying quantum gravity. In particular, holographic correspondences associated with boundary conformal field theories (BCFT), CFT defined on a manifold with boundaries, have attracted much attention in recent years. The reason is that a BCFT has two equivalent gravity duals. The first one is obtained by introducing an end-of-the-world brane, which plays the role of the boundary on the gravity side, to the gravity side of standard AdS/CFT. The correspondence between the first gravity dual and the BCFT is called AdS/BCFT. The second gravity dual is obtained by applying the Karch-Randall brane-world holography to the first one, which will result in a dynamical AdS gravity coupled to a non-gravitational region. Such an equivalence between three theories is called double holography. The novel point of double holography is one can observe non-perturbative quantum effects in the second gravity dual while keeping the first gravity dual classical. Therefore, in this framework, one can use tools from both BCFT and classical gravity to study the quantum effects of gravity.

As a field theory, the BCFT ends at the boundary (the end of the world). However, by comparing the BCFT and its second gravity dual, it looks like quantum gravity arises from and goes beyond the end of the world. In this dissertation, we study several aspects and developments of AdS/BCFT and double holography. We start with setups with timelike boundaries. We will first introduce a conformal map method to study dynamics associated with moving boundaries, the so-called moving mirror setups, in 2D CFT. We will also explain how studies of black holes using moving mirrors in old days can be related to recent developments of the island formula via AdS/BCFT and double holography. Then we will move on to a new holographic setup called wedge holography, which is realized by introducing two parallel end-of-the-world branes in the gravity dual of AdS/BCFT. While a wedge-like region is left on the gravity side, this construction causes a dimensional reduction on the field theory side and results in a codimension-two holography. After that, we focus on the causal structures in double holography. In particular, we show that the causality in BCFT is protected, but that in the second gravity dual is broken in a certain way for consistency. Then we will move on to introduce a new quantum informational quantity called pseudo entropy, which is a generalization of entanglement entropy to post-selection setups. We will end up discussing BCFT with spacelike boundaries where pseudo entropy naturally appears. We will see how AdS/BCFT provides not only a tool for analyzing setups with spacelike boundaries but also a strong motivation related to dS holography for doing so.

Contents

1 Introduction and Summary

As one of the most ancient subjects, the aim of theoretical physics is clear and simple. Theoretical physicists attempt to use languages as simple as possible to explain their observations of nature, describe how the universe runs, and efficiently make correct predictions of the real world. Such a language turns out to be a theoretical model. Since we only have one real world, or at least we usually assume so, the developments of theoretical physics usually come along with unifications of different models into a new one that consistently includes old ones. The unification of gravity and spacetime curvature into general relativity by Einstein is a good example. General relativity, together with quantum theory, are two of the most important ingredients in modern physics established in the early 20th century.

In the theoretical physics of the 21st century, one of the most important yet challenging problems is to construct a theory of quantum gravity, which is a unification of quantum theory and gravity described by general relativity, and give testable predictions from it. Nowadays, the holographic principle [1, 2] plays a significant role in the studies of quantum gravity. The holographic principle states that a theory of quantum gravity, even though we do not know how to precisely describe it, should be equivalent to a lower dimensional non-gravitational quantum theory. The most well-studied example is the equivalence between quantum gravity in a $(d+1)$-dimensional asymptotically anti-de Sitter spacetime (AdS) and a d-dimensional conformal field theory (CFT) living on its boundary, the so-called AdS/CFT correspondence [3]. Here, AdS is a spacetime with a negative cosmological constant, and CFT is a class of quantum theory that describes certain many-body systems. Once the precise correspondences between AdS and CFT are perfectly revealed, one will be able to use well-understood non-gravitational quantum theory to formulate and analyze mysterious quantum gravity. In other words, the problem of quantum gravity will be automatically solved. Therefore, working on understanding AdS/CFT better is a crucial key to exploring quantum gravity.

Despite its great success, there are still many big issues with the current stage of studies on quantum gravity using AdS/CFT. First, although AdS/CFT is in principle a correspondence between quantum AdS gravity and CFT, it is examined almost only in the classical limit. The classical limit is a special case where gravity is effectively described by general relativity. Second, even at the classical AdS limit, the dictionary that tells us which object in AdS corresponds to which object in CFT is not completely understood. Third, according to

experimental observations, our universe has a small but positive cosmological constant and is hence well-approximated by de Sitter spacetime (dS) but not AdS. However, holography associated with dS [4, 5] is much less well-understood.

In this dissertation, we will focus on two main topics which play crucial roles in solving the above issues recently.

The first topic is a generalization of AdS/CFT called AdS/BCFT [6, 7]. Here, BCFT stands for boundary CFT [8], which is CFT defined on a manifold with boundaries. In general, the presence of boundaries will break the conformal symmetries holden by the original CFT. Therefore, we consider boundary conditions that maximally preserve conformal symmetries for BCFT. In other words, BCFT describes a world where there is an end of space. Corresponding to the boundaries on the BCFT side, its AdS gravity dual should also contain objects that play a role of boundaries. In standard bottom-up approaches [6,7] of the AdS/BCFT correspondence, such "boundaries" are realized by the so-called end-of-the-world branes, which are dynamical codimension-1 objects. So far, it seems that AdS/BCFT is just a straightforward extension of AdS/CFT. The reason why AdS/BCFT is getting more and more attention in studying quantum gravity is because it admits another alternative but equivalent "intermediate" description which captures quantum features of gravity [9]. The intermediate description is a setup in which an AdS gravity is coupled to a non-gravitational heat bath. The correspondence between the intermediate description and the fully gravitational description in the higher dimension has been known as the Karch-Randall holography [9] in a different context. The novel equivalence between these three descriptions is called double holography [10], and it has opened a window to study quantum gravity. One example in which the application of double holography played an important role is the discovery of the island formula [10], which partially resolves the information paradox proposed by Hawking in 1970s [11–13] in a series of recent progress on this problem [14–18].

The second topic is the application of quantum information methods to AdS/CFT. Nowadays, quantum information is becoming a common language in different fields of theoretical physics including high energy theory and condensed matter theory. Starting from the discovery of the Ryu-Takayanagi formula [19,20], which relates geometric quantities in AdS gravity and the entanglement entropy in CFT, quantum information methods have been playing important roles in expanding the AdS/CFT dictionary. This is very natural since AdS/CFT is an equivalence between two quantum theories, which means the dictionary is about how

the quantum information on the one side is encoded on the other side.

After presenting some basics on these topics, we study several different aspects of them [21–29]. The topics treated in this dissertation are summarized as follows.

Moving Mirrors and Hawking Radiation (Chapter 3)

Moving mirror models [30] are quantum field theories defined on manifolds with a moving boundary. While there is no dynamical gravity involved in these models, it is known that certain moving mirrors can mimic Hawking radiation. It is easy to intuitively understand this point if one considers a free scalar field. In this case, the outgoing wave will experience a Doppler effect while the ingoing wave will not. Therefore, a moving mirror will emit thermal radiation. However, it is not clear how a moving mirror model can be regarded as a black hole background with dynamical gravity.

We extend the BCFT formulation to those with moving boundaries in 2-dimension and compute physical quantities such as the energy-stress tensor and entanglement entropy in these setups. We will also show that, with the help of AdS/BCFT and double holography, one can indeed relate moving mirror setups to those with dynamical gravity coupled to a heat bath. These are exactly the setups where the island formula [10] is discovered. In this sense, we show how the old idea of moving mirrors is equivalent to the new idea of the island model.

This part is based on our publications [24, 25].

Wedge Holography (Chapter 4)

In the AdS/BCFT correspondence, the gravity side contains end-of-the-world branes in it. The branes enrich the physics one can possibly realize. We consider combining two branes in a certain way in the AdS/BCFT correspondence. More precisely, we take the two branes to be parallel to each other and keep the distance between them as a constant. Then, in this case, the asymptotic boundary of the AdS spacetime will experience a dimensional reduction, i.e. it will lose one dimension. Therefore, by combining two branes in this way, we can realize a codimension-2 holography, in the sense that the BCFT_d reduces to CFT_{d-1} while the gravity side is kept to be always $(d+1)$-dimension. Since the gravity side in this case looks like a wedge, we call such a setup wedge holography. The wedge holography provides a new construction of holographic correspondence and contributes to many aspects of the study of both holography and quantum gravity.

This part is based on our publication [22].

Causal Structures in Double Holography (Chapter 5)

The causal structure is always one nontrivial point to check in a boundary-bulk type duality. Let us take the AdS/CFT correspondence as an example. The CFT is defined on the asymptotic boundary of the AdS spacetime. In this case, for the AdS/CFT to be consistent, two points which are spacelike separated on the boundary should not be causally connected in the bulk, otherwise, the causality of the boundary theory, i.e. the CFT, would be broken. However, this statement is a rather nontrivial one if one forgets about AdS/CFT and only looks at the AdS gravity, and it needs to be shown without any inputs from AdS/CFT. Indeed, this has been already shown to be true under some reasonable assumptions [31, 32].

On the other hand, for a given bulk-boundary type duality which is not well understood, studying the causal structure will help us know more about the duality. We study the causal structure in double holography. Double holography, as a correspondence between three equivalent pictures, includes at least two bulk-boundary type dualities: AdS/BCFT and the Karch-Randall holography. We show that the causal structure in the higher dimensional bulk is compatible with the causality on the BCFT side in AdS/BCFT. However, in the Karch-Randall holography, there exist causal shortcuts in the bulk, which means that the corresponding boundary theory has an intrinsic nonlocality. We will also discuss the physical consequences of the phenomenon observed here.

This part is based on our publication [27].

Pseudo Entropy and its Application (Chapter 6)

The Ryu-Takayanagi formula [19, 20] relates certain codimension-2 surfaces in the AdS gravity with the entanglement entropy on the CFT side. However, one may wonder what is the corresponding object on the CFT side of more general codimension-2 surfaces. Motivated by this question, we generalize the notion of entanglement entropy to post-selection setups, and propose a new quantum informational quantity called pseudo entropy. After revealing the basic properties of pseudo entropy in general quantum systems, we will study the behavior of pseudo entropy in quantum many-body systems and see that it is useful when discussing quantum phase transition.

This part is based on our publication [21, 23, 26].

Spacelike Boundaries, dS Branes and Holography (Chapter 7)

The notion of BCFT is formulated on Euclidean manifolds with boundaries or Lorentzian manifolds with timelike boundaries. However, one may wonder what if we have spacelike boundaries. This kind of setup is hard to treat with conventional technics of BCFT. Besides, at the first glance, it seems that we do not have a strong motivation to study such setups. The situation turns out to be different when one takes holography into consideration. The gravity dual of a Lorentzian BCFT_d with a timelike boundary corresponds to an AdS_{d+1} with an end-of-the-world brane which turns out to be AdS_d. This is related to AdS brane-world holography. On the other hand, if one changes the boundary of the BCFT into a spacelike one, the end-of-the-world-brane in the AdS_{d+1} bulk will turn into a dS_d brane, and is related to dS brane-world holography [33, 34]. Therefore, studying the extensions of BCFT with spacelike boundaries is expected to open a window to the dS holography.

We examine such cases and explain how holography provides a route to extend BCFT to those with spacelike boundaries. We will also study the holographic pseudo entropy associated with such setups. This part is based on our publication [22].

2 Backgrounds and Preliminaries

In this chapter, we review the background knowledge of this dissertation. We will start from the boundary conformal field theories [8] and then move on to AdS/BCFT [6, 7]. Related to this, we will also review the Karch-Randall brane-world holography [9] and see how they are combined into the so-called double holography [10]. At the end of this chapter, we will review the basics of entanglement entropy, and how they are computed in holographic setups [19,20]. We will mainly focus on the case where the dimension on the field theory side is 2, and that on the gravity side is 3. When we talk about the results in general dimensions, we will denote the dimension as d and $d+1$, respectively.

2.1 Boundary Conformal Field Theory

In this section, we review some basic perspectives of boundary conformal field theories. For simplicity, we will consider Euclidean formulations in this section. Corresponding Lorentzian setups can be obtained straightforwardly via analytic continuation.

Boundary conformal field theories (BCFT) [8] are conformal field theories that are defined on manifolds with boundaries, but not all such theories are BCFT. The existence of boundaries will break conformal symmetries holden by the original CFT, but only those maximally preserve the conformal symmetries are called BCFT. In 2D, it is known that the following boundary condition

$$T(z) - \bar{T}(\bar{z}) = 0, \tag{2.1}$$

can maximally preserve the conformal symmetries. Here, $T(z)$ ($\bar{T}(z)$) is the chiral (anti-chiral) part of the energy-stress tensor. This boundary condition is often called the Cardy boundary condition [8].

In a standard CFT, all the information can be determined by the conformal symmetry and the following three ingredients: the central charge c, the conformal weights of the primary operators, and the operator product expansion (OPE) coefficients between them [35]. In a BCFT, besides these ingredients inherited from the original CFT, there are also some new ingredients due to the existence of the boundary. The first one is the partition function evaluated on the unit disk with radius 1,

$$g = \langle \mathbb{I} \rangle_{\text{disk}} \,. \tag{2.2}$$

Here, $\mathbb{I}$ is the identity operator. The disk partition function is often called the g function and reflects the property of the boundary condition a. For later convenience, let us introduce the boundary entropy S_{bdy} as

$$S_{\text{bdy}} = \log g. \tag{2.3}$$

Moreover, besides the primary operators inherited from the original CFT, those living on the boundaries should be treated separately. These two sets of operators are called the bulk primaries and the boundary primaries respectively. As a result, besides OPE coefficients inherited from the original CFT, one should also have the coefficients when expanding the product of two boundary operators with the sum of boundary operators, and those when expanding one bulk operator with the sum of boundary operators.

An important feature of BCFT is that the correlation functions in a BCFT can be computed using the so-called doubling trick or mirror method [8]. For example, if we consider a BCFT defined on an upper half plane (UHP) $\text{Im}z \geq 0$, then the correlation function of a local operator $\mathcal{O}(z = z_0, \bar{z} = \bar{z}_0)$ which can be decomposed into the chiral part and the antichiral part as

$$\mathcal{O}(z = z_0, \bar{z} = \bar{z}_0) = \mathcal{O}(z = z_0)\bar{\mathcal{O}}(\bar{z} = \bar{z}_0), \tag{2.4}$$

can be computed in the following way:

$$\langle \mathcal{O}(z = z_0, \bar{z} = \bar{z}_0) \rangle_{\text{UHP}} \propto \langle \mathcal{O}(z = z_0)\bar{\mathcal{O}}(z = \bar{z}_0) \rangle_{\mathbb{C}} \,. \tag{2.5}$$

In other words, we can regard the boundary as a mirror that maps the antichiral part on the UHP to the chiral part on the lower half plane, and compute the chiral correlation functions on the whole plane $\mathbb{C}$. This holds also for multi-point functions. For more general manifolds other than UHP, one can simply use the conformal map to relate it to an UHP and then get the answer.

2.2 The AdS/BCFT Correspondence

The AdS/BCFT correspondence [6, 7] is a bottom-up construction of the gravity dual of BCFT. In this section, we review the basic construction of AdS/BCFT. Considering the usage of AdS/BCFT in this dissertation, we use the Lorentzian signature in this section.

Consider a BCFT defined on a manifold Σ with timelike boundaries $\partial\Sigma$. In the AdS/BCFT construction, the action of the gravity dual is given by

$$I_{\text{bulk}} = \frac{1}{16\pi G_N}\int_{\mathcal{M}}\sqrt{-g}(R-2\Lambda) + \frac{1}{8\pi G_N}\int_{\Sigma}\sqrt{-\gamma}B + \frac{1}{8\pi G_N}\int_{Q}\sqrt{-h}(-K-T). \quad (2.6)$$

Here, $(\mathcal{M}, g_{\mu\nu})$ is the gravity dual, which is a portion of a $(d+1)$-dimensional asymptotically AdS spacetime (AAdS). Its boundary contains two parts $\partial\mathcal{M} = \Sigma \cup Q$ with $\partial\Sigma = \partial Q$. Besides the standard asymptotic boundary Σ on which the BCFT is defined, Q is a new ingredient appearing in AdS/BCFT and is called an end-of-the-world brane. $g_{\mu\nu}$, γ_{ij} and h_{ab} are metrics of $\mathcal{M}$, Σ and Q, respectively. B_{ij} and K_{ab} are the extrinsic curvatures of Σ and Q, respectively. Note that here our convention of normal vectors is to let the normal vector of Σ point toward the outside of $\mathcal{M}$, while the normal vector of Q points toward the inside of $\mathcal{M}$. T is a parameter called the tension of Q, which roughly corresponds to the mass of the end-of-the-world brane. While both Σ and Q are boundaries of $\mathcal{M}$, their difference is as follows. Taking the variation with respect to the boundary term, we have

$$\delta I_{\text{bulk}} = \frac{1}{16\pi G_N}\int_{\Sigma}\sqrt{-\gamma}\ \delta\gamma^{ij}(B_{ij} - B\gamma_{ij}). \quad (2.7)$$

There are two choices to let the variation be zero. One is to take $\delta\gamma^{ij} = 0$, and another one is to take $(B_{ij} - B\gamma_{ij}) = 0$. These two boundary conditions are called the Dirichlet boundary condition and the Neumann boundary condition, respectively. On Σ, we impose the Dirichlet boundary condition. The variation at the vicinity of Q looks very similar, but we take the Neumann boundary condition on Q instead. The precise boundary condition turns out to be

$$K_{ab} - Kh_{ab} - Th_{ab} = 0. \quad (2.8)$$

While we need to in general consider quantum gravity, i.e. the gravitational path integral over all possible configurations, in the bulk theory, we can approximate the whole path integral with an on-shell configuration in the semiclassical limit $G_N \to 0$. This is the regime we are going to consider. See figure 1 for a sketch of the AdS/BCFT correspondence.

2.3 Karch-Randall Brane-world and Double Holography

In the spirit of holographic principle [1,2], it is considered that a gravitational theory should be equivalent to some theory on its "boundary". However, there are no strict requirements

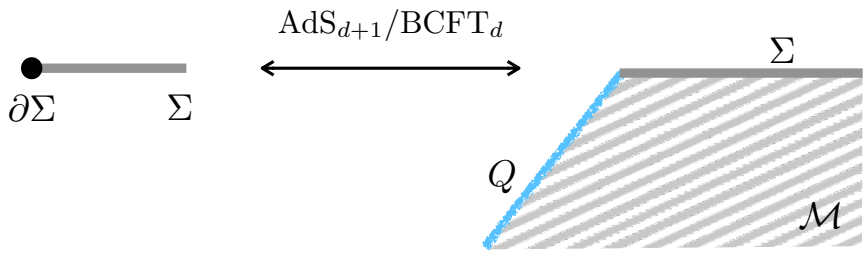

Figure 1: A sketch of the AdS/BCFT correspondence. The left figure shows a BCFT defined on a manifold Σ with a boundary $\partial\Sigma$. The right figure shows its gravity dual $\mathcal{M}$, which is a portion of AdS, where the boundary condition imposed on the asymptotic boundary Σ is Dirichlet, and that imposed on the end-of-the-world brane Q is Neumann.

on how the "boundary" is chosen. In the previous section, we have seen that an on-shell configuration $\mathcal{M}$ of (2.6) is considered to be equivalent to a BCFT defined on Σ, the asymptotic boundary of $\mathcal{M}$. Let us now consider an alternative way of choosing the boundary, which will lead us to the Karch-Randall brane-world holography [9, 36, 37]. See figure 2 for a sketch of the Karch-Randall brane-world holography.

More specifically, let us take the entire $\partial\mathcal{M} = Q \cup \Sigma$ as the boundary. In this case, since the boundary condition imposed on Q is the Neumann boundary condition and that imposed on Σ is Dirichlet, the boundary theory in this case turns out to be a dynamical gravity living on Q coupled to a non-gravitational theory living on Σ. Because of the existence of dynamical gravity on the brane, this setup is called the brane-world. Besides the existence of gravity, there exists a common CFT living on the whole boundary $\Sigma \cup Q$. Different from the gravity sector, the matter sector, i.e. the CFT, can freely transfer from one side of Q and Σ to the other side [38]. We will not write down the effective action [39, 40] in the brane-world theory since it is complicated and will not be used in this dissertation. We would like to note that one intriguing feature in the Karch-Randall brane-world is that the graviton living on Q is massive [9, 41].

Till now, we have seen that constructing the gravity dual of BCFT in a bottom-up way leads to the bulk theory given by (2.6). At the same time, this bulk theory can be dual to another theory where a gravitational theory couples to a non-gravitational theory via the

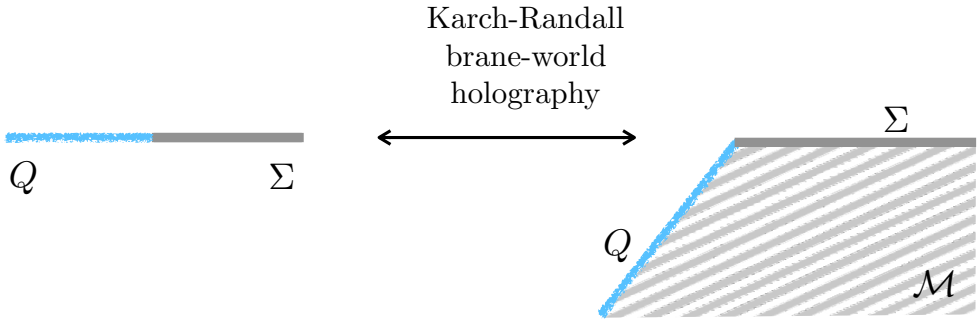

Figure 2: A sketch of the Karch-Randall brane-world holography. The right figure shows the higher dimensional dual $\mathcal{M}$ where the Dirichlet boundary condition is imposed on the asymptotic boundary Σ and the Neumann boundary condition is imposed on the end-of-the-world brane Q. The left figure shows the boundary dual, where a dynamical gravity on Q is attached to a non-gravitational theory on Σ.

Karch-Randall brane-world holography. Therefore, we now have three equivalent pictures in this setup. The equivalence between these three pictures is called double holography [10]. In this dissertation, when discussing double holography, we will use "BCFT picture" to refer to the BCFT, "bulk picture" to refer to the bulk gravity theory, and "intermediate picture" to refer to the brane-world theory in the Karch-Randall holography. The reason why we call the last description the "intermediate picture", is because it can be obtained from the BCFT picture by partially applying holography. A useful intuition is that, if we divide the BCFT_d defined on Σ into the $\partial\Sigma$ part and the $\Sigma\backslash\partial\Sigma$ part, then the former part will roughly be a CFT_{d-1}. Accordingly, we can apply $\text{AdS}_d/\text{CFT}_{d-1}$ to map it to a AdS_d. In the end, we will get a theory where a dynamical gravity is attached to a non-gravitational theory, which is nothing but is the boundary theory in the Karch-Randall brane-world holography. However, note that this intuition is not exactly precise, since the degrees of freedom on the boundary are nontrivially interacting with those in the bulk.

The terminology "double holography" was firstly used in [10], where the authors considered a black hole living on the brane and emitting Hawking radiation to the non-gravitational heat bath. They related this setup to the bulk picture and the BCFT picture equivalent to it, used them to analyze the Hawking radiation, and got an answer which is consistent with

the unitarity. In other words, they performed the analysis without having an information paradox [11–13]. This analysis leads to the discovery of the island formula [10, 16–18], which is one of the most important progress with respect to the black hole information paradox in recent years.

2.4 Entanglement Entropy in AdS/CFT and AdS/BCFT

Entanglement is a crucial feature in quantum systems [42]. Let us consider an arbitrary quantum system, and divide it into two parts A and B. Then, the whole Hilbert space is given by the tensor product $\mathcal{H}_A \otimes \mathcal{H}_B$. When the whole system is in a pure state, the von Neumann entropy of the reduced density matrix on subsystem A

$$S(\rho_A) = -\mathrm{Tr}(\rho_A \log \rho_A), \tag{2.9}$$

is known to be a good quantity to count the amount of entanglement between A and B [43]. Therefore, the von Neumann entropy in this case is often called the entanglement entropy. In fact, entanglement entropy is not a good quantity to count the amount of entanglement when the whole system is in a mixed state. However, we will still call it the "entanglement entropy".

It is in general difficult to compute the entanglement entropy in a quantum field theory [44–46]. However, for holographic CFTs with classical holographic duals, there is a simple way. For a CFT state with a static classical geometric dual, the entanglement entropy of the subsystem A can be calculated as

$$S(\rho_A) = \frac{\text{Area of } \gamma_A}{4G_N} \tag{2.10}$$

where G_N is the Newton constant and γ_A is a codimension-2 surface lying on the time slice of AdS whose boundary is the CFT state we are focusing on and satisfies:

- Its boundary coincides with the boundary of A, i.e $\partial\gamma_A = \partial A$.
- It is homologous to A, i.e. it can be obtained from A by a continuous deformation.
- It gives the minimal area.

This result is known as the Ryu-Takayanagi formula [19, 20], which was at first a conjecture and then proven in [47]. Such γ_A is called the Ryu-Takayanagi surface. The RT formula

suggests that the entanglement in quantum many-body systems is related to the geometry in the bulk spacetime. This surprising finding initiates the study of holography using quantum information. See [48] for generalization to time-dependent cases. See [49, 50] for quantum corrections on the RT formula.

Since we will mainly focus on AdS/BCFT in this dissertation, we would also like to see how the entanglement entropy is computed in this case. In fact, the modification, in this case, is simple. All we need to do is to regard the end-of-the-world brane as one point in the homology condition. In other words, we allow the RT surface to end on the brane in AdS/BCFT. In practice, we can firstly find the minimal connected surface which does not end on the brane and the minimal disconnected surface which ends on the brane, and then take the smaller one between them. This recipe is conjectured in [6, 7] and proven for some special cases in [51].

3 Moving Mirrors and Hawking Radiation

In this chapter, we analyze a class of quantum field theories defined on manifolds with boundaries moving in time. These kinds of theories are often called the moving mirror models [30]. For simplicity, we will focus on moving mirror models in 2D CFT. In this case, we can apply conformal map methods to relate them to standard setups of BCFT, which greatly simplifies analyses.

We will also consider the holographic dual associated with the moving mirror models. In old days, moving mirror models are considered as toy models of Hawking radiation [11–13], since the energy stress tensor emitted by certain moving mirrors is exactly the same as that of the standard Hawking radiation from a black hole [30]. However, on the other hand, moving mirror models are just toy models without dynamical gravity involved. To this end, we will see that moving mirror models can actually be naturally related to island models in the context of AdS/BCFT and double holography.

This chapter is based on our publications [24, 25].

3.1 Conformal Map Method

Let us consider a 2D CFT defined on a manifold with a moving boundary and introduce the following light cone coordinates

$$(u, v) = (t - x, t + x), \tag{3.1}$$

to parameterize the spacetime. We denote the trajectory of the moving mirror as

$$x = Z(t), \tag{3.2}$$

and consider the right hand side, i.e. the $x \geq Z(t)$ side, as the physical region. Consider the following conformal map to relate it to another manifold whose light cone coordinates $(\tilde{u}, \tilde{v})$ are related to (u, v) via

$$(\tilde{u}, \tilde{v}) = (p(u), v). \tag{3.3}$$

The new theory is defined on another manifold with another moving boundary in general. Here, we consider the special case where the boundary in the $(\tilde{u}, \tilde{v})$ coordinate is static, i.e., the boundary trajectory is given by

$$\tilde{x} = \frac{1}{2}(-\tilde{u} + \tilde{v}) = 0. \tag{3.4}$$

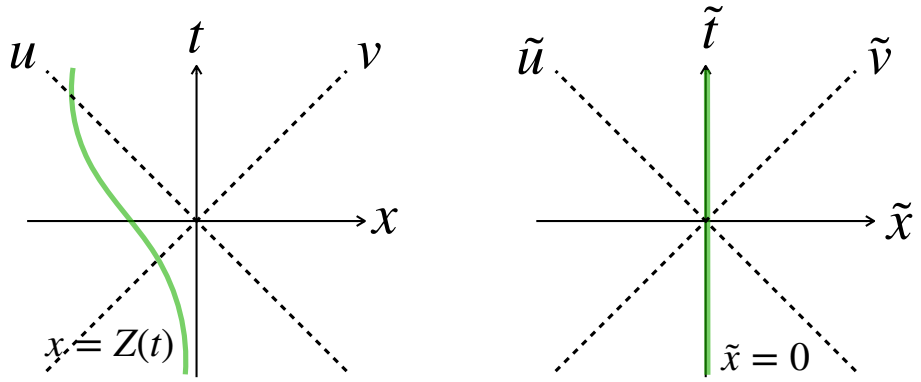

Figure 3: A sketch of the conformal map method in moving mirror setups. The left figure shows a generic moving mirror setup where the mirror trajectory $x = Z(t)$ is shown in green. The physical region is taken to be $x \geq Z(t)$. By using a conformal map, we can map it into the setup shown in the right figure, where the mirror is static.

See figure 3 for a sketch. In this case, it is easy to find that the original mirror trajectory $x = Z(t)$ and the conformal map can be related in the following way.

$$p(t - Z(t)) = t + Z(t). \tag{3.5}$$

We can also introduce $f(u) \equiv p^{-1}(u)$, with which we will have

$$Z\left(\frac{\tilde{u} + f(\tilde{u})}{2}\right) = \frac{\tilde{u} - f(\tilde{u})}{2}, \qquad Z\left(\frac{u + p(u)}{2}\right) = \frac{p(u) - u}{2}. \tag{3.6}$$

In this special case, the path integral defined on the new manifold parameterized by $(\tilde{u}, \tilde{v})$ is nothing but a standard BCFT defined on a half plane. As a result, the state realized by this path integral is just the vacuum state on a half-infinite line. The energy stress tensor is hence given by $T_{\tilde{u}\tilde{u}} = T_{\tilde{v}\tilde{v}} = 0$. Therefore, we can simply apply the conformal map to find that the energy stress tensor in the original setup is given by

$$T_{uu} = -\frac{c}{24\pi}\{p(u), u\} = -\frac{c}{24\pi}\left(\frac{p'''(u)}{p'(u)} - \frac{3}{2}\left(\frac{p''(u)}{p'(u)}\right)^2\right), \tag{3.7}$$

where c is the central charge of the CFT.

3.2 Computation of the Entanglement Entropy

Let us then move on to see how to compute the entanglement entropy in the moving mirror setups via the conformal map method. In an ordinary 2D CFT, the n-th Rényi entropy of a single interval $A = [x_1, x_2]$ can be evaluated from the correlation functions of twist operators as following [45, 46]

$$S_A^{(n)} = \frac{1}{1-n} \log\langle \sigma_n(t, x_1)\bar{\sigma}_n(t, x_2)\rangle, \tag{3.8}$$

where the conformal weights of the twist operators $\sigma_n(t, x_0)$ and $\bar{\sigma}_n(t, x_1)$ are given by $h_n = \bar{h}_n = \frac{c}{24}\left(n - \frac{1}{n}\right)$. Once the n-th Rényi entropy is successfully computed, we can take the $n \to 1$ to get the entanglement entropy. With the conformal map considered above, we can map the moving mirror setup to the right half plane (RHP) of $\mathbb{R}^{1,1}$, which allows us to easily evaluate the correlation functions of the twist operators. More precisely, we have

$$\langle \sigma_n(t, x_1)\bar{\sigma}_n(t, x_2)\rangle = \langle \tilde{\sigma}_n\left(\tilde{t}_1, \tilde{x}_1\right) \tilde{\bar{\sigma}}_n\left(\tilde{t}_2, \tilde{x}_2\right)\rangle_{\text{RHP}} \times \left(p'(u_1)p'(u_2)\right)^{h_n}. \tag{3.9}$$

Fortunately, the two point functions are much easier to evaluate on a right half plane. Let us present the result in holographic CFT.

The two point functions of twist operators in a holographic BCFT can be approximated in the following way [52]

$$\langle \tilde{\sigma}_n\left(\tilde{t}_1, \tilde{x}_1\right) \tilde{\bar{\sigma}}_n\left(\tilde{t}_2, \tilde{x}_2\right)\rangle_{\text{RHP}} = \max\begin{cases} \langle \tilde{\sigma}_n\left(\tilde{t}_1, \tilde{x}_1\right) \tilde{\bar{\sigma}}_n\left(\tilde{t}_2, \tilde{x}_2\right)\rangle_{\mathbb{R}^{1,1}} \\ g^{2(1-n)}\langle \tilde{\sigma}_n\left(\tilde{t}_1, \tilde{x}_1\right) \tilde{\bar{\sigma}}_n\left(\tilde{t}_1, -\tilde{x}_1\right)\rangle_{\mathbb{R}^{1,1}}^{1/2}\langle \tilde{\sigma}_n\left(\tilde{t}_2, \tilde{x}_2\right) \tilde{\bar{\sigma}}_n\left(\tilde{t}_2, -\tilde{x}_2\right)\rangle_{\mathbb{R}^{1,1}}^{1/2} \end{cases}. \tag{3.10}$$

The candidate of the entanglement entropy evaluated from the first channel is called the connected entanglement entropy, S_A^{con}, and that evaluated from the second channel is called the disconnected entanglement entropy, S_A^{dis}, respectively. As a result, the true entanglement entropy is given by $S_A = \min\left[S_A^{\text{con}}, S_A^{\text{dis}}\right]$. The corresponding computation on the AdS side is to find the connected RT surface and the disconnected RT surface, and then take the smaller one between them, as we have explained in section 2.4.

3.3 Escaping Mirror

As the first example, we consider the following conformal map:

$$p(u) = -\beta \log(1 + e^{-u/\beta}). \tag{3.11}$$

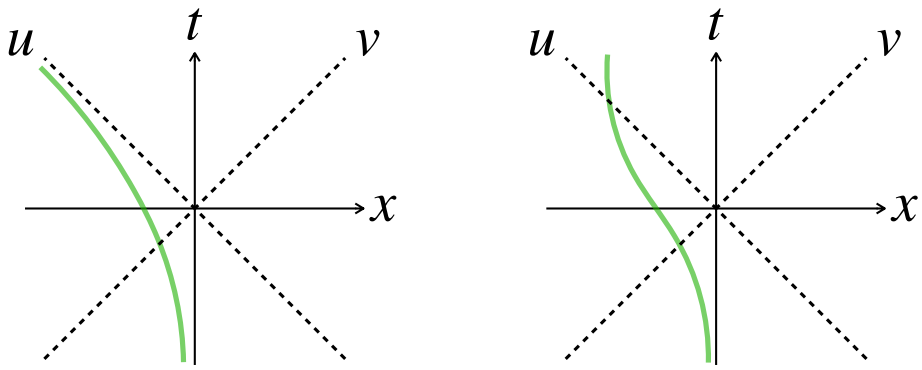

Figure 4: Escaping mirror (left) and kink mirror (right).

Here β is a positive constant which can be interpreted as the temperature of the radiation emitted by the moving mirror, as we will see below.

At the early time limit $u \to -\infty$, we have $p(u) \simeq u$, which means that the mirror is static $Z(t) \simeq 0$ in the early time. On the other hand, it is also important to look at the asymptotic behavior at $u \to \infty$ where we have

$$p(u) \simeq -\beta e^{-u/\beta}, \tag{3.12}$$

and hence

$$Z \simeq -t - \beta e^{-2t/\beta}. \tag{3.13}$$

Therefore, the mirror moves towards the left hand side and approaches the speed of light exponentially. From this feature, we call it the escaping mirror. See the left of figure 4 for a sketch.

In this case, the energy stress tensor turns out to be

$$T_{uu} = \frac{c}{48\pi\beta^2}\left(1 - \frac{1}{(1+e^{u/\beta})^2}\right). \tag{3.14}$$

One can easily find from this expression that the late time limit is given by $T_{uu} \simeq \frac{c}{48\pi\beta^2}$. This is similar to the energy stress tensor of a thermal density matrix with temperature $\frac{1}{2\pi\beta}$. Thus, we know how the constant β is related to the inverse temperature.

Let us then divide the whole system into the mirror part and the other part A, and consider the entanglement entropy between them. If A has a fixed end point at $x = a$, the

entanglement entropy at late time $t \to \infty$ looks like

$$S_A \simeq \frac{c}{12\beta}(t-a) + \frac{c}{6}\log\frac{t}{\epsilon} + S_{\rm bdy}, \tag{3.15}$$

where c is the central charge of the underlying CFT, ϵ is a UV cutoff corresponding to the lattice distance, and $S_{\rm bdy}$ is the boundary entropy. When we let the edge of the subsystem A to be comoving with the mirror at $x = -t + \alpha$ where α is sufficiently small, then at late time

$$S_A \simeq \frac{c}{6\beta}t + \frac{c}{6}\log\frac{\alpha}{\epsilon} + S_{\rm bdy}. \tag{3.16}$$

In both cases, the entanglement entropy grows monotonically in the escaping mirror setup.

3.4 Kink Mirror

Let us consider another example with

$$p(u) = \beta\log(1+e^{(u-u_0)/\beta}) - \beta\log(1+e^{-u/\beta}). \tag{3.17}$$

Here, β and u_0 are positive constants.

To grasp the feature of this mirror profile, it is useful to look at the $\beta \to 0$ limit. At this limit, one can see that the mirror is static $Z(t) = 0$ at early time $t < 0$. Then it moves at the speed of light $Z(t) = -t$ at the intermediate time $0 \le t \le u_0/2$. Finally, it will stop and turns back to be static $Z(t) = -u_0/2$ at $t > u_0/2$. See the right of figure 4 for a sketch.

Accordingly, we call such a moving mirror the kink mirror. Let us compute the time evolution of the entanglement entropy also in this case. For simplicity, we consider holographic CFT. We consider a subsystem which comoves with the mirror trajectory. See figure 5 for a plot of it. We can see in this case the entanglement entropy follows a Page curve [13], i.e. it firstly grows and finally goes back at late time. In this case, unitarity is manifest since we are just considering a standard quantum field theory. However, it is not obvious how this setup is related to a setup with dynamical gravity. In the next section, we will see this relation can be given by considering holography associated with moving mirrors.

3.5 Connection to Island Models

In this section, we explain how moving mirrors can be related to island models where dynamical gravity is coupled to a non-gravitational heat bath. Let us consider a holographic

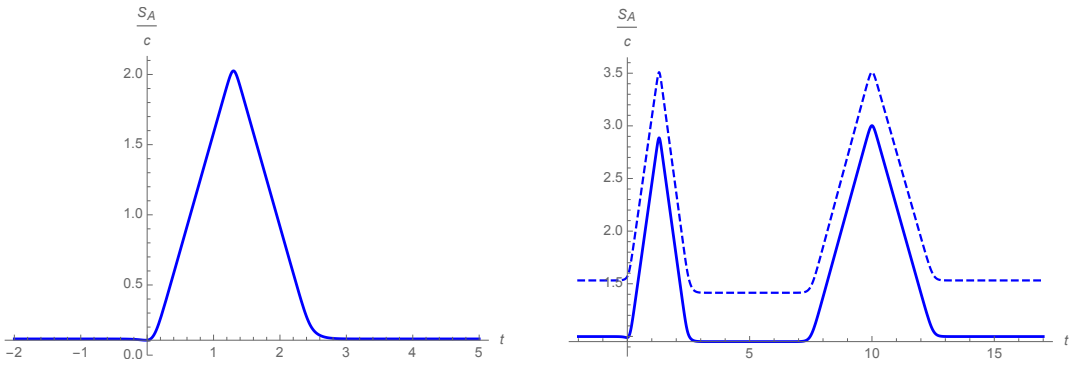

Figure 5: Time evolution of entanglement entropy in a kink mirror setup. The left figure shows the case for $A = [Z(t) + 0.1, \infty]$ and the right figure shows the case for $A = [Z(t) + 0.1, Z(t)+10]$. The solid curve and the dashed curve correspond to S_A^{dis} and S_A^{con}, respectively. Here, we set $\beta = 0.1, u_0 = 5$, $\epsilon = 0.1$ and $S_{\text{bdy}} = 0$. The plots are taken from figure 6 in our publication [24].

CFT with a moving mirror. As we have shown at the beginning of this chapter, one can always use a conformal map to map the moving mirror setup to a right half plane. Since we already know the gravity dual of the right half plane (See section 2.2), it is straightforward to get the gravity dual of a moving mirror, where the end-of-the-world brane moves in the bulk spacetime and back reacts on it. If we further apply the Karch-Randall holography, we can get another description where a dynamical gravity living on the brane is coupled to the heat bath and emits radiation into it. This is exactly the setup of the island models [10]. In this way, we are able to get an equivalent gravitational theory to the moving mirror setups.

4 Wedge Holography

In this chapter, we propose a novel holographic correspondence called wedge holography. This is based on our publication [22]. Wedge holography is a codimension-2 holographic correspondence found by combining ingredients in AdS/BCFT. Therefore, we will firstly introduce a useful coordinate to discuss AdS/BCFT and also wedge holography. Then we will present the statement of wedge holography, and give a brief derivation from AdS/BCFT. After that, we will compute several quantities from the bulk side of wedge holography, and see how these results reflect the features of the expected boundary dual.

4.1 Basic Statements of Wedge Holography

In this section, after introducing some coordinates which are useful for us to discuss the wedge holography, we present the basic statements of it. Let us start with the Poincaré AdS_{d+1} whose metric is given by

$$ds^2 = L^2 \left(\frac{dz^2 - dt^2 + dx^2 + \sum_{i=1}^{d-2} d\xi_i^2}{z^2} \right). \tag{4.1}$$

It is useful to introduce the following coordinate transformation

$$z = \frac{y}{\cosh(\rho/L)}, \tag{4.2}$$

$$x = y\tanh(\rho/L). \tag{4.3}$$

In the new coordinate, the metric of the Poincaré AdS can be rewritten as

$$ds^2 = d\rho^2 + L^2\cosh^2\frac{\rho}{L} \left(\frac{dy^2 - dt^2 + \sum_{i=1}^{d-2} d\xi_i^2}{y^2} \right). \tag{4.4}$$

Let us firstly consider introducing one end-of-the-world brane in this coordinate. As we have already reviewed in the preliminaries, the boundary condition imposed on the brane is

$$K_{ab} - Kh_{ab} - Th_{ab} = 0. \tag{4.5}$$

By solving this equation, it is straightforward to find out that the brane profile is given by

$$\rho = \rho_* \tag{4.6}$$

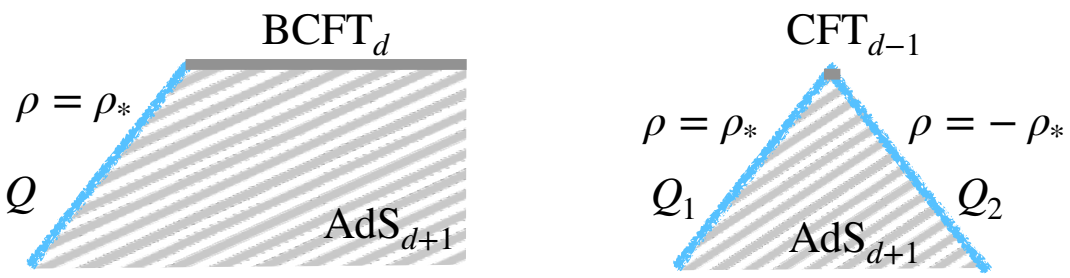

Figure 6: A standard AdS/BCFT with one brane (left) and a wedge holography setup with two branes (right).

where ρ_* is a constant which relates to the tension T via

$$T = \frac{d-1}{L}\tanh(\rho_*/L). \tag{4.7}$$

See the left of figure 6 for a sketch.

Let us then move on to consider introducing two branes in our setups. Let us introduce a brane Q_1 at $\rho = \rho_*$ and a brane Q_2 at $\rho = -\rho_*$. As a result, the bulk AdS$_{d+1}$ region turns out to be a wedge-like region W_{d+1} surrounded by Q_1 and Q_2. The physical region of the bulk is given by $-\rho_* \leq \rho \leq \rho_*$. Here we would like to note that although the region W_{d+1} looks like a wedge, the two branes are parallel to each other and the distance does not change when moving along the z direction or the y direction. However, we will still call it the wedge region.

On the other hand, the boundary side experiences a dimensional reduction. When we have only one brane, it is a BCFT$_d$. However in the current case, it is a CFT$_{d-1}$. The UV cutoff of CFT inherits from the geometric cutoff $z \geq \epsilon$ on the bulk gravity side. See the right of figure 6 for a sketch.

Within this setup, we can consider the following double holography-like correspondence. First of all, we have a classical gravity living in the $d+1$ dimensional wedge region. The boundary condition imposed on Q_1 and Q_2 is Neumann, and that imposed on the asymptotic boundary Σ is Dirichlet. As the first step, this classical gravity should be equivalent to a quantum field theory defined on Σ. This is effectively a CFT$_{d-1}$. In other words, we have a codimension-two holography associated with this wedge region. On the other hand,

in the spirit of the brane-world holography [9, 33, 34], we can instead regard $Q_1 \cup Q_2$ as the boundary of the wedge region. Since the boundary conditions imposed on them are Neumann, it corresponds to a brane-world gravity defined on both Q_1 and Q_2, which are joint with each other through the interface Σ. Since the brane-world gravity is expected to reflect the quantum nature of gravity even when the bulk gravity is classical, we may summarize the argument here as follows:

$$\begin{aligned} & \text{Classical gravity in the wedge-like } \mathrm{AdS}_{d+1}, \\ \simeq\ & \text{(Quantum) brane-world gravity on two pieces of } \mathrm{AdS}_d\ (= Q_1 \cup Q_2), \\ \simeq\ & \mathrm{CFT}_{d-1} \text{ on } \Sigma. \end{aligned} \tag{4.8}$$

We can also argue this in an alternative way. We can apply the brane-world holography first to the classical gravity in the bulk. As a result, we have quantum AdS_d gravity on the two branes Q_1 and Q_2. Since both of Q_1 and Q_2 share the same asymptotic boundary Σ, then both of them should be equivalent to some CFT defined on Σ according to the AdS/CFT correspondence. In the end, we obtain the codimension-two holography which connects the bulk classical gravity and the CFT on the boundary.

4.2 Deriving Wedge Holography from AdS/BCFT

Let us then present a more careful way to derive the codimension-two holography described above. We are going to do so by taking a proper limit of AdS/BCFT.

Starting from a BCFT_d defined on a d dimensional strip with width l. Let us denote the finite direction as x and restrict it to $0 \leq x \leq l$. According to the AdS/BCFT construction, there are two ways to construct its gravity dual. In the first construction, there is one single brane which connects the two boundaries of the BCFT. On the other hand, in the second construction, one have two branes in the bulk gravity which correspond to the two boundaries of the BCFT, respectively. If both of the constructions are allowed, then the true gravity dual is given by the one which gives the minimal free energy. However, if the boundary conditions on the two boundaries are different from each other, then only the second construction is allowed. We consider the latter situation, and take the tension of the two branes to be the same. As a result, now we have a BCFT_d defined on a d dimensional strip, and we also have its gravity dual in which there are two end-of-the-world branes Q_1 and Q_2 corresponding to the two boundaries of the BCFT. The next step is to take the limit $l \to 0$, which brings the

d dimensional strip to a $(d-1)$ dimensional flat spacetime. On the bulk gravity side, the $\mathrm{AdS}_d + 1$ is now reduced to the wedge geometry shown in the right of figure 6.

The argument above provides a derivation of the codimension-two holography we presented in the previous section.

4.3 Holographic Free Energy

From now on, let us compute some CFT_{d-1} quantity from the wedge AdS_{d+1} gravity dual we presented above. As the very first example, let us consider the free energy. The free energy F is defined as the minus log of the CFT partition function,

$$F = -\log Z_{\mathrm{CFT}}. \tag{4.9}$$

According to the GKPW dictionary [53, 54], this can be translated to the gravity side as

$$F = -\log Z_{\mathrm{grav.}} \simeq \log e^{-I_{\mathrm{grav.}}[\mathcal{M}]} = I_{\mathrm{grav.}}[\mathcal{M}], \tag{4.10}$$

where $\mathcal{M}$ is the most dominating on-shell configuration on the gravity side, and we have used the semiclassical approximation when evaluating the partition function of the gravitational path integral. Therefore, the holographic free energy is nothing but just the bulk gravity action evaluated in the most dominating on-shell configuration. In this case, the gravitational action is given by

$$I_{\mathrm{grav.}} = -\frac{1}{16\pi G_N}\int_{\mathcal{M}}\sqrt{g}(R-2\Lambda) - \frac{1}{8\pi G_N}\int_{Q_1\cup Q_2}\sqrt{h}(K-T) - \frac{1}{8\pi G_N}\int_{\Sigma}\sqrt{\gamma}B. \tag{4.11}$$

where the first term is the Einstein-Hilbert term, the second term is the Gibbons-Hawking term on Q_1 and Q_2, and the third term is the Gibbons-Hawking term on the asymptotic boundary Σ. Note that here in this section, the convention for the normal vectors to Q (and hence the extrinsic curvature K) is opposite to that used in section 2.2.

Since we are considering the Poincaré metric, and the two end-of-the-world branes lie at $\rho = \pm\rho_*$, respectively, it is straightforward to find that the Riemann curvature is

$$R = -d(d+1)/L^2, \tag{4.12}$$

and the cosmological constant is

$$\Lambda = -d(d+1)/2L^2. \tag{4.13}$$

On the other hand, for the quantities evaluated on the branes, the extrinsic curvature is

$$K = (d/L)\tanh(\rho_*/L), \tag{4.14}$$

and the brane tension is

$$T = ((d-1)/L)\tanh(\rho_*/L). \tag{4.15}$$

Finally, the extrinsic curvature evaluated on the asymptotic boundary Σ is

$$B = d/L. \tag{4.16}$$

Plugging all these into the gravitational action, we have

$$\begin{aligned} I_{\text{grav.}} &= \frac{d \cdot V_{d-1} L^{d-2}}{4\pi G_N} \int_0^{\rho_*} d\rho \left(\cosh\frac{\rho}{L}\right)^d \int_{\epsilon\cosh\frac{\rho}{L}}^{\infty} \frac{dy}{y^d} - \frac{L^{d-1} V_{d-1} \tanh\frac{\rho_*}{L}}{4\pi G_N} \left(\cosh\frac{\rho_*}{L}\right)^d \int_{\epsilon\cosh\frac{\rho_*}{L}}^{\infty} \frac{dy}{y^d} \\ &\quad - \frac{d \cdot L^{d-1} V_{d-1} \sinh\frac{\rho_*}{L}}{4\pi G_N \epsilon^{d-1}} \qquad (4.17) \\ &= \frac{V_{d-1} L^{d-1}}{4\pi G_N \epsilon^{d-1}} \left[\frac{d}{(d-1)L} \int_0^{\rho_*} d\rho \cosh\frac{\rho}{L} - \frac{1}{d-1} \sinh\frac{\rho_*}{L} - d\sinh\frac{\rho_*}{L} \right] \\ &= \frac{(1-d) \cdot V_{d-1} L^{d-1}}{4\pi G_N \epsilon^{d-1}} \sinh\frac{\rho_*}{L} \qquad (4.18) \end{aligned}$$

where the volume element V_{d-1} is defined as

$$V_{d-1} = \int dt_E d\xi_1 \cdots d\xi_{d-2}. \tag{4.19}$$

Now let us have a quick check if this result is consistent with the conjecture that the $d+1$ dimensional wedge region we are considering corresponds to a $d-1$ dimensional CFT. The holographic free energy we computed here scales as $V_{d-1}\epsilon^{1-d}$, which is known as the free energy of a vacuum CFT state in $d-1$ dimension. In this sense, the holographic free energy passed our first consistency check.

4.4 Holographic Entanglement Entropy

Another useful quantity to evaluate is entanglement entropy. Now, since our CFT is a $d-1$ dimensional theory, we would like to take a time slice which is $d-2$ dimension, and consider a subsystem A on it. To see how the entanglement entropy should be computed holographically from the AdS_{d+1} side, let us go back to the AdS/BCFT setup where we have not yet taken

the width-goes-to-zero limit of the BCFT$_d$. Accordingly, the region A is uplifted into a $d-1$ dimensional region which may be denoted as $A \times [0, l]$.

The reason why we would like to uplift the CFT$_{d-1}$ back to a BCFT$_d$ is because we already know how to compute the holographic entanglement entropy in standard AdS/BCFT. What we need to do is to find the $d-1$ dimensional minimal surface which is homologous to $A\times[0, l]$ in the bulk spacetime, which may ends on the end-of-the-world branes, since each brane is regarded to be one point in the homology condition.

Obviously, this structure is protected when one takes the width of the BCFT to 0. As a result, when one wants to compute the holographic entanglement entropy for a $d-2$ dimensional subregion A defined on the CFT$_{d-1}$, all one need to do is to find the $d-1$ dimensional minimal surface which intersects the asymptotic boundary Σ such that the intersection is A.

In practice, we can first fix the end regions of the $d-1$ dimensional surface on Q_1 and Q_2, find the minimal one with respect to the fixed end regions, and then vary the end-regions to get the global minimum. Let us call this $d-1$ dimensional surface Γ_A, and call its intersection with the brane Q_i as $\gamma_A^{(i)}$. From the above explanation, the holographic entanglement entropy for the subregion A can be evaluated as

$$S_A = \min_{\gamma_A \ s.t.\ \partial\gamma_A^{(1)}=\partial\gamma_A^{(2)}=\partial A} \left[\min_{\Gamma_A \ s.t.\ \partial\Gamma_A=\gamma_A^{(1)}\cup\gamma_A^{(2)}} \left[\frac{A(\Gamma_A)}{4G_N} \right] \right]. \tag{4.20}$$

in wedge holography.

Before explicitly evaluating this holographic entanglement entropy for specific setups, it is worth noting some general properties of this expression. First, because of the geometric nature of this formula, and because we are taking the minimum over all possible surfaces, this geometric quantity satisfies the inequalities satisfied by general entanglement entropy, such as subadditivity and strong subadditivity. Second, although we just discussed the static case above, it is also straightforward to extend this formula to Lorentzian cases which are not time-independent. All we need to do is replace the minimalization above with firstly finding all the extremal values and then finding the minimal among all of them, just as what one does in the standard HRT formula case [48].

Let us then move on to compute the holographic entanglement entropy in concrete examples. For simplicity, let us take A as a $d-2$ dimensional round disk $\sum_{i=1}^{d-2} \xi_i^2 \leq R^2$ where R is the radius. In general, in order to find the correct minimal surface, we need to solve

complicated partial differential equations. However, we will see that the computation can be greatly simplified in this special case.

To see this, let us firstly make a guess at the $\rho_* \ll L$ limit. At this limit, the wedge is so thin such that it can be roughly regarded as a direct product of an AdS_d and $-\rho_* \leq \rho \leq \rho_*$, since the warp factor can be approximated as a constant at this limit. In this case, one can immediately find that the minimal surface can be written as $x^2 + z^2 + \sum_{i=1}^{d-2}(\xi_i)^2 = R^2$. In other words, the minimal surface is a part of the sphere which is sandwiched by the two branes. It might be more simple if we write the sphere using the $(y, \rho, ...)$ coordinate, with which the sphere is given by

$$y + \sum_{i=1}^{d-2}(\xi_i)^2 = R^2. \tag{4.21}$$

From the above argument, we know that the minimal surface is given by (4.21) for small ρ_*. This serves as a good guess for general ρ_*. In fact, we are going to see that (4.21) is the minimal surface we are looking even for general ρ_*. To see this, let us work in the $d = 3$ case. We are working on this case just to avoid complicated formulae, and the argument can be generalized to general d. Let us make a perturbation given by $y = \sqrt{l^2 - \xi^2} + f(\xi, \rho)$ to see if the sphere is robust against it. Here, we impose $f(\pm l, \rho) = 0$. This is because that the surface should end on the boundary of subsystem A in CFT_{d-1}. After a complicated computation, we find that the area of the sphere Γ_A turns out to be

$$\begin{aligned}
&\mathrm{Area}(\Gamma_A) \\
&= -\left[\frac{L\cosh\frac{\rho}{L}\xi f(\xi)}{R(R^2-\xi^2)^{\frac{1}{2}}}\right]_{\xi=-R}^{\xi=R} \\
&\quad + \int d\rho d\xi \left[\frac{LR\cosh\frac{\rho}{L}}{R^2-\xi^2}\right. \\
&\quad \left. + \frac{L\cosh\frac{\rho}{L}}{2R^3(R^2-\xi^2)^2}\left(2R^4f^2 + L^2R^2\left(\cosh^2\frac{\rho}{L}\right)(R^2-\xi^2)(\partial_\rho f)^2 + 2R^2\xi(R^2-\xi^2)f\partial_\xi f + (R^2-\xi^2)^3(\partial_\xi f)^2\right)\right]
\end{aligned} \tag{4.22}$$

From this exact expression, we can confirm that the minimum is realized when $y + \sum_{i=1}^{d-2}(\xi_i)^2 = R^2$, i.e. when the surface is a sphere.

Based on the argument above, let us now evaluate the area of the minimal surface, i.e. the partial square sandwiched by the two branes. Then we will find that the holographic

entanglement entropy is given by

$$S_A = \frac{\text{Area}(\Gamma_A)}{4G_N} = \text{Vol}(S^{d-3}) \cdot \frac{L^{d-2}}{2G_N} \cdot \int_0^{\rho_*} d\rho \left(\cosh\frac{\rho}{L}\right)^{d-2} \cdot \int_{\epsilon\cosh\frac{\rho}{L}}^{R} dy \frac{R(R^2-y^2)^{\frac{d}{2}-2}}{y^{d-2}}, \quad (4.23)$$

Here $\text{Vol}(S^{d-3})$ is the volume of a unit radius $d-3$ dimensional sphere, which is given by $\text{Vol}(S^{d-3}) = \frac{2\pi^{\frac{d-2}{2}}}{\Gamma\left(\frac{d-2}{2}\right)}$.

Let us again consider the limit $\rho_*/L \ll 1$ which simplifies the situation. In this case, the HEE turns out to be

$$S_A = \frac{\text{Area}(\Gamma_A)}{4G_N} \simeq \frac{\rho_*}{4G_N} \cdot \left[\text{Area}(\gamma_A^{(1)}) + \text{Area}(\gamma_A^{(2)})\right], \quad (4.24)$$

where

$$\text{Area}(\gamma_A^{(1)}) = \text{Area}(\gamma_A^{(2)}) = L^{d-2} \cdot \text{Vol}(S^{d-1}) \cdot \int_\epsilon^R dy \frac{R(R^2-y^2)^{\frac{d}{2}-2}}{y^{d-2}}. \quad (4.25)$$

This has the same form with the standard holographic entanglement entropy evaluated from the standard $\text{AdS}_d/\text{CFT}_{d-1}$ correspondence. In fact, if one performs the identification $\frac{\rho_*}{G_N} \simeq \frac{1}{G_N^{(d)}}$, then they match exactly with each other.

From now on, we would like to work on the finite ρ_* case by perform the integral straightforwardly. Since it is difficult to do it exactly, we will work on the series expansion with respect to R/ϵ. First of all,

$$\begin{aligned}
&\int_{\epsilon\cosh\frac{\rho}{L}}^{R} dy \frac{R(R^2-y^2)^{\frac{d}{2}-2}}{y^{d-2}} \\
=&p_1\left(\cosh\frac{\rho}{L}\right)^{-d+3}\left(\frac{R}{\epsilon}\right)^{d-3} + p_3\left(\cosh\frac{\rho}{L}\right)^{-d+5}\left(\frac{R}{\epsilon}\right)^{d-5} + \cdots \\
&\ldots + \begin{cases} p_{d-3}\left(\cosh\frac{\rho}{L}\right)^{-1}\left(\frac{R}{\epsilon}\right) + p_{d-2} + \mathcal{O}\left(\frac{\epsilon}{R}\right) & d: \text{ even} \\ p_{d-4}\left(\cosh\frac{\rho}{L}\right)^{-2}\left(\frac{R}{\epsilon}\right)^2 + q\log\left(\frac{R}{\epsilon}\right) + \mathcal{O}(1) & d: \text{ odd} \end{cases} \quad (4.26) \\
=&\begin{cases} \sum_{k=1}^{(d-2)/2} p_{2k-1}\left(\cosh\frac{\rho}{L}\right)^{-d+2k+1}\left(\frac{\epsilon}{R}\right)^{d-2k-1} + p_{d-2} + \mathcal{O}\left(\frac{\epsilon}{R}\right) & d: \text{ even} \\ \sum_{k=1}^{(d-3)/2} p_{2k-1}\left(\cosh\frac{\rho}{L}\right)^{-d+2k+1}\left(\frac{\epsilon}{R}\right)^{d-2k-1} + q\log\left(\frac{R}{\epsilon}\right) + \mathcal{O}(1), & d: \text{ odd} \end{cases} \quad (4.27)
\end{aligned}$$

where the coefficients are as follows:

$$\begin{aligned}
&p_1 = (d-3)^{-1}, p_3 = -(d-4)/[2(d-5)], \cdots \\
&p_{d-2} = (2\sqrt{\pi})^{-1}\Gamma((d-2)/2)\Gamma((3-d)/2) \quad (\text{if } d \text{ is even}), \\
&q = \frac{\sqrt{\pi}}{\Gamma((4-d)/2)\Gamma((d-1)/2)} \quad (\text{if } d \text{ is odd}).
\end{aligned} \quad (4.28)$$

As a result, we have

$$S_A = \frac{\text{Area}(\Gamma_A)}{4G_N} = \frac{L^{d-2}}{2G_N}\cdot \text{Vol}(S^{d-3})\int_0^{\rho_*} d\rho \left(\cosh\frac{\rho}{L}\right)^{d-2}\cdot \int_{\epsilon\cosh\frac{\rho}{L}}^{R} dy \frac{R(R^2-y^2)^{\frac{d}{2}-2}}{y^{d-2}},$$
$$= \frac{\pi^{\frac{d-2}{2}}L^{d-1}}{G_N\Gamma\left(\frac{d-2}{2}\right)}\left(\frac{\sinh\frac{\rho_*}{L}}{d-3}\left(\frac{R}{\epsilon}\right)^{d-3} - \frac{(d-4)}{2(d-5)}\left(\frac{\sinh\frac{3\rho_*}{L}}{12}+\frac{3\sinh\frac{\rho_*}{L}}{4}\right)\left(\frac{R}{\epsilon}\right)^{d-5}+\cdots\right.$$
$$\left.\cdots + \begin{cases} p_{d-2}\int_0^{\rho_*/L} d\eta\,(\cosh\eta)^{d-2} + \mathcal{O}\left(\frac{\epsilon}{R}\right), & d: \text{ even} \\ q\int_0^{\rho_*/L} d\eta\,(\cosh\eta)^{d-2}\cdot\log\left(\frac{R}{\epsilon}\right)+\mathcal{O}(1), & d: \text{ odd} \end{cases}\right). \quad (4.29)$$

There are some key observations with respect to this result. The first point is that the scaling behavior of HEE evaluated here agrees with general results [20,55] in $d-1$ dimensional CFTs. Moreover, by comparing this result with that in the standard $\text{AdS}_d/\text{CFT}_{d-1}$, one can find

$$\frac{1}{G_N^{(d)}} = \frac{1}{G_N}\int_0^{\rho_*} d\rho \left(\cosh\frac{\rho}{L}\right)^{d-2}. \quad (4.30)$$

These observations give consistency checks on the conjecture that the wedge region in AdS_{d+1} should be equivalent to a CFT_{d-1} on the asymptotic boundary.

Let us list some low dimensional results explicitly. For $d=3$, i.e. the $\text{AdS}_4/\text{CFT}_2$ case,

$$S_A = \frac{L^2}{G_N^{(4)}}\sinh\frac{\rho_*}{L}\log\frac{R}{\epsilon}+\mathcal{O}(1), \quad (4.31)$$

For $d=4$, i.e the $\text{AdS}_5/\text{CFT}_3$ case, we have

$$S_A = \left(\frac{\pi L^3}{G_N^{(5)}}\sinh\frac{\rho_*}{L}\right)\frac{R}{\epsilon} - \frac{\pi L^3}{G_N^{(5)}}\left(\frac{1}{2}\frac{\rho_*}{L}+\frac{1}{4}\sinh\frac{2\rho_*}{L}\right)+\mathcal{O}\left(\frac{\epsilon}{R}\right). \quad (4.32)$$

For $d=5$, i.e the $\text{AdS}_6/\text{CFT}_4$ case, we obtain

$$S_A = \left(\frac{\pi L^4}{G_N^{(6)}}\sinh\frac{\rho_*}{L}\right)\left(\frac{R}{\epsilon}\right)^2 - \frac{\pi L^4}{G_N^{(6)}}\left(\frac{\sinh\frac{3\rho_*}{L}}{12}+\frac{3\sinh\frac{\rho_*}{L}}{4}\right)\log\frac{R}{\epsilon}+\mathcal{O}(1). \quad (4.33)$$

All of these have the expected scaling behavior which support the idea of wedge holography.

4.5 Viewing from the d-dimensional Brane-world Gravity

Till now, we have focused on the holographic computation including holographic free energy and holographic entanglement entropy from the AdS_{d+1} gravity side. From now on, we would like to have a glance on what happens in the d-dimensional brane-world point of view. While

the exact gravitational action on the brane-world [39] is complicated, the leading order is expected to be the Einstein-Hilbert term. From the equivalence between the gravitational path integral in AdS_{d+1} and that in the AdS_d brane-world, under the saddle point approximation, we have

$$\frac{1}{16\pi G_N}\int_{\mathrm{AdS}_{d+1}}\sqrt{g}R=\frac{2}{16\pi G_N^{(d)}}\int_{\mathrm{AdS}_d}\sqrt{g^{(d)}}R^{(d)}, \tag{4.34}$$

where the prefactor 2 on the right hand side comes from the fact that we now have two brane-worlds Q_1 and Q_2.

On the other hand, by decomposing the integral in AdS_{d+1} into the ρ direction and other directions, we can write the left hand side as

$$\frac{1}{16\pi G_N}\int_{\mathrm{AdS}_{d+1}}\sqrt{g}R=\frac{1}{16\pi G_N}\int_{-\rho_*}^{\rho_*}d\rho\left(\cosh\frac{\rho}{L}\right)^{d-2}\int_{\mathrm{AdS}_d}\sqrt{g^{(d)}}R^{(d)}. \tag{4.35}$$

By comparing these two equations, we get the following expression for the effective Newton constant in the brane-world gravity:

$$\frac{1}{G_N^{(d)}}=\frac{1}{G_N}\int_0^{\rho_*}d\rho\left(\cosh\frac{\rho}{L}\right)^{d-2}. \tag{4.36}$$

While it is complicated to evaluate this integral, it would be useful to study some asymptotic behavior of it. When ρ_* is small compared to L, i.e. $\rho_*/L\ll 1$, we have $G_N/(LG_N^{(d)})\simeq\rho_*/L+((d-2)/6)(\rho_*/L)^3+\ldots$. We would like to note that this behavior agrees with the one we obtained from the HEE evaluation. On the other hand, if ρ_* is large compared to L, i.e. $\rho_*/L\gg 1$, then we have $G_N/(LG_N^{(d)})\simeq(2^{2-d}/(d-2))e^{(d-2)\rho_*/L}\gg 1$.

We can observe that the Newton constant becomes small when the brane tension is large, which corresponds to the semiclassical limit of the brane-world gravity. Let us keep this simple qualitative relation in mind.

4.6 Applications and Developments of Wedge Holography

Since our proposal of wedge holography, it has been applied to study different physical phenomena and has been generalized to various situations.

A key feature in the standard Karch-Randall brane-world holography where one only has one brane is that the graviton in the intermediate picture acquires a nontrivial mass [9, 41]. However, since graviton in Einstein gravity is massless, one may wonder if important results

obtained from the standard double holography such as the island formula [10] will still hold or not. The authors of [56] address this question using the setup of wedge holography. The reason for that is because, in the intermediate picture of wedge holography, there is no non-gravitational region and the graviton mass is zero. Besides this application, the wedge holography has also been generalized into different situations [57–59]. Indeed, wedge holography is a powerful toy model for analyzing different phenomena.

5 Causal Structures in Double Holography

In this chapter, we discuss the causal structure in AdS/BCFT and Karch-Randall braneworld holography. We will first review why studying the causal structure is important using an example in the AdS/CFT correspondence. Then we will summarize our main results and show the derivations. This chapter is based on a part of [27].

5.1 Compatibility of Causality in the AdS/CFT Correspondence

Consider an AAdS_{d+1} spacetime $\mathcal{M}$ and denote its asymptotic boundary as Σ. Let us consider two points $p, q \in \Sigma$. On the CFT side, since the CFT is a local QFT, one can send a signal from p to q if and only if q is at the causal future of p. On the other hand, one question we can ask is that if one can send a signal from p to q through $\mathcal{M}$ while p and q are spacelike separated. From the expectation of the AdS/CFT correspondence, the answer is of course no. However, this is a rather nontrivial statement on the AdS gravity side. Let us summarize it as a statement. This statement is taken from statement A from our publication [27].

Statement A (Compatibility of Causality in AdS/CFT)**.**

In the AdS/CFT correspondence, for any two points $p, q \in \Sigma = \partial\mathcal{M}$, if p and q are not causally connected on the asymptotic boundary Σ, then they are not causally connected in the bulk $\mathcal{M}$ either.

When $\mathcal{M}$ is a global AdS, it is straightforward to check the statement A is true. In more complicated situations, statement A is guaranteed by the Gao-Wald theorem [31]. Here, we take this from theorem A.0 in our publication [27].

Theorem A.0 (Gao-Wald theorem)**.**

Let $(\mathcal{M}, g_{\mu\nu})$ be a spacetime with a timelike boundary $\partial\mathcal{M} = \Sigma$ at asymptotic infinity. Suppose $(\mathcal{M}, g_{\mu\nu})$ satisfies the following four conditions:

1. *$\mathcal{M}$ is a solution of the Einstein equation in which the matter sector satisfies averaged null energy condition (ANEC),*
2. *Null generic condition,*
3. *$\bar{\mathcal{M}} \equiv \mathcal{M} \cup \Sigma$ is strongly causal (strong causality condition),*

4. $J^+_{\bar{\mathcal{M}}}(p) \cap J^-_{\bar{\mathcal{M}}}(q)$ *is compact for any* $p, q \in \mathcal{M}$.

Let $A_\Sigma(p, \mathcal{M})$ *be*

$$A_\Sigma(p,\mathcal{M}) \equiv \{r \in \Sigma | \textit{there exists a future directed causal curve } \lambda \\ \textit{which starts from } p \textit{ and ends at } r \textit{ satisfying } \lambda - (p \cup r) \subset \mathcal{M} \ \} \ , \tag{5.1}$$

then for $p \in \Sigma$ *and* $\forall q \in \partial A_\Sigma(p, \mathcal{M})$, q *satisfies* $q \in J^+_{\bar{\mathcal{M}}}(p) \backslash I^+_{\bar{\mathcal{M}}}(p)$. *Moreover, any causal curve connecting* p *and* q *lies entirely in* Σ, *and hence it is also a null geodesic on* (Σ, γ_{ij}), *i.e.* $q \in J^+_\Sigma(p) \backslash I^+_\Sigma(p)$. *Here,* $J^+_{\mathcal{N}}(p)$ $(I^+_{\mathcal{N}}(p))$ *is the causal (chronological) future of* p *on the manifold* $\mathcal{N}$.

The ANEC appearing in the first condition states that the energy-stress tensor $T_{\mu\nu}$ satisfies

$$\int_l T_{\mu\nu} k^\mu k^\nu \geq 0 \ , \tag{5.2}$$

for any null curve l where k^μ is the tangent vector of l. The null generic condition means that every null geodesic in $\mathcal{M}$ contains a point such that

$$k^\mu k^\nu k_{[\rho} R_{\sigma]\mu\nu[\alpha} k_{\beta]} \neq 0 \ . \tag{5.3}$$

These two conditions lead to the existence of the conjugate points for any null geodesic [32,60]. It is worth noting that global AdS does not satisfy the null generic condition. Therefore, global AdS is not covered by the Gao-Wald theorem, and we need to treat it separately.

The strong causality condition means that, for any point $p \in \bar{\mathcal{M}}$, every neighborhood of p contains another neighborhood of p which no causal curve can intersect more than once. Roughly, it means that no causal curve in $\bar{\mathcal{M}}$ is almost closed.

One consequence of the Gao-Wald theorem is

$$\partial A_\Sigma(p, \mathcal{M}) \ \subseteq \ J^+_\Sigma(p) \backslash I^+_\Sigma(p). \tag{5.4}$$

Here, since $\partial A_\Sigma(p, \mathcal{M})$ bounds the region which can receive a signal through the bulk $\mathcal{M}$, and $J^+_\Sigma(p) \backslash I^+_\Sigma(p)$ bounds the region which can receive a signal through the asymptotic boundary Σ, the Gao-Wald theorem leads to the statement A.

Let us repeat the logic of the results shown in this section. The causality condition and the consistency of the AdS/CFT correspondence suggests that statement A should be true.

However, statement A itself is very nontrivial on the AdS gravity side. Therefore, we need to check it on the gravity side independent from the inputs from AdS/CFT correspondence. If it is confirmed on the gravity side, then it provides a nontrivial check to AdS/CFT. On the other hand, if one found counter examples of statement A on the gravity side, that would mean either causality in the CFT or the AdS/CFT correspondence itself was broken.

In the following, we will study the causal structure in double holography (i.e. AdS/BCFT correspondence and Karch-Randall brane-world holography).

5.2 Results in Double Holography

In this section, we summarize the results we get for double holography. As the setup, we consider an AAdS spacetime $\mathcal{M}$ with an end-of-the-world brane Q in it. Here, we require $\mathcal{M}$ to be a on-shell configuration with the action (2.6). This $\mathcal{M}$ gives us the bulk picture in the double holography. It corresponds to a BCFT defined on its asymptotic boundary Σ, i.e. the BCFT picture, via the AdS/BCFT correspondence. At the same time, it also corresponds to a dynamical gravity defined on Q coupled to a heat bath on Σ, i.e. the intermediate picture, via the Karch-Randall brane-world holography. The results are listed below.

Statement B. *Let Σ be compatible with a BCFT. For any two points $p, q \in \Sigma$, if p and q are not causally connected on the asymptotic boundary Σ, then they are not causally connected in the bulk $\mathcal{M}$ either.*

Statement C. *For any two points $p, q \in Q$, if p and q are not causally connected on the end-of-the-world brane Q, then they are not causally connected in the bulk $\mathcal{M}$ either.*

Statement D. *Two points $p \in \Sigma$ and $q \in Q$ can be causally connected in the bulk $\mathcal{M}$, even if they are not causally connected on $\partial\mathcal{M} = \Sigma \cup Q$.*

Here, these three statements are taken from statement B, C, D in our publication [27], respectively.

We will prove these statements in the following sections, but we would like to first comment on the physical consequences of these statements, based on the logic explained in the previous section.

First of all, statement B implies that the causal structure in the bulk picture is compatible with the causality in the BCFT picture. This is nontrivial since the AdS/BCFT correspon-

dence is just a bottom-up construction and we do not know to what extent it should hold. Therefore, this result gives another strong support to the AdS/BCFT construction.

Second, statement B, C, D together imply that, in order for the effective theory in the intermediate picture to be compatible with the bulk picture, it need to have a special causal structure. Specifically, if one wants to send a signal within the gravitational region Q or the non-gravitational heat bath Σ, then there is no causal short cut in the bulk. However, if one wants to send a signal between Q and Σ, then one can always find a causal short cut in the bulk. This will lead to several significant consequences in the Karch-Randall brane-world holography. We will comment on this at the end of this chapter.

5.3 Explicit Checks in the Vacuum Configuration

We consider the vacuum configuration of (2.6) in this section and explicitly check that statement B, C, D hold in this case. We will focus on AdS_3 for simplicity. Extensions to higher dimensions are straightforward.

A pure AdS_3 is given by

$$ds^2 = -(r^2+1)d\tau^2 + \frac{dr^2}{r^2+1} + r^2 d\phi^2 \tag{5.5}$$

in the global coordinate where $-\pi < \phi \leq \pi$. The location of the end-of-the-world brane with tension Q is given by

$$r\cos\phi = \frac{T}{\sqrt{1-T^2}}. \tag{5.6}$$

The physical region in the bulk is the region surrounded by the brane Q and the asymptotic boundary. When the brane tension is positive (negative), then the larger (smaller) portion of the bulk is taken. See figure 7 for a sketch. It would be useful to introduce an alternative coordinate system as

$$\sinh\rho = r\cos\phi, \tag{5.7}$$

$$\cosh^2\rho\,\cosh^2\eta = 1 + r^2. \tag{5.8}$$

with which the metric is

$$ds^2 = d\rho^2 + \cosh^2\rho\left(-\cosh^2\eta\; d\tau^2 + d\eta^2\right). \tag{5.9}$$

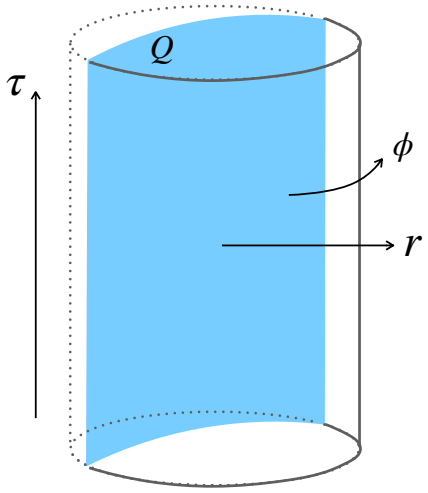

Figure 7: A sketch of the AdS_3 vacuum. The end of the world brane Q is shaded blue. The bulk region $\mathcal{M}$ is the region surrounded by Q and the asymptotic boundary.

and the brane profile is

$$\rho = \text{arctanh}(T) \equiv \rho_*. \tag{5.10}$$

This coordinate will be useful when we discuss the causal structure in pure AdS_3.

The first step to discuss the causal structure is to write down the null geodesics. Then the causal diamonds can be accordingly found. Let us consider a lightray launching from $(\tau, r, \phi) = (-\pi/2, \infty, -\pi/2)$. There are infinitely many such geodesics but any of them can be written as the intersection between the hypersurface $\rho = \text{const.}$ and $\tau = 2\arctan\left(\tanh\frac{\eta}{2}\right)$. Also, we can find all these geodesics do not only share the starting point but also share the endpoint at $(\tau, r, \phi) = (\pi/2, \infty, \pi/2)$. Besides, if we take $\rho \to \pm\infty$, then we can get the null geodesics on the asymptotic boundary. See figure 8 for a sketch.

Because all the null geodesics in pure AdS intersect the asymptotic boundary and the current setup has a translation symmetry with respect to the ϕ direction. The above information is sufficient for us to know all about the causal structure in pure AdS. As a quick check, we can immediately find that the following statement is true. This statement is taken from statement A.1 in our publication [27].

Statement A.1. *Consider pure AdS_3. Let p be a spacetime point with $p : (\tau, r, \phi) = (\tau_p, \infty, \phi_p)$ and $\mathcal{R}$ be an observer localized at $(r, \phi) = (\infty, \phi_{\mathcal{R}})$ on the asymptotic bound-*

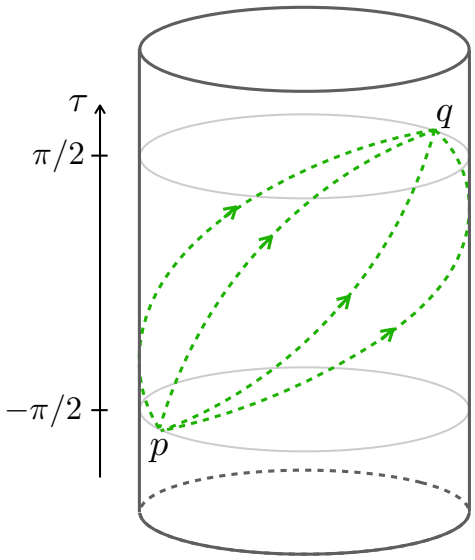

Figure 8: Some null geodesics launching from $p : (\tau, r, \phi) = (-\pi/2, \infty, -\pi/2)$ in global AdS_3. These geodesics are in green. All of them reach the same point at the same time.

ary. Consider sending a signal at the speed of light from p to the observer $\mathcal{R}$. Then $\Delta\tau_{\text{asym}} = \Delta\tau_{\text{bulk}}$, where $\Delta\tau_{\text{asym}}$ ($\Delta\tau_{\text{bulk}}$) is the required time on the asymptotic boundary (in the bulk) for receiver $\mathcal{R}$ to observe the emitted light ray.

The point is that, if we consider sending a signal between antipodal points in the spatial sense, then although there exists infinitely many bulk geodesics which are as fast as the null geodesic on the asymptotic boundary, there exists no one strictly faster. On the other hand, if the one that sends the signal and the one that receives the signal are not antipodal points, then there do not even exist bulk geodesics which are as fast as the one on the asymptotic boundary.

This is different from the case which is referred to by the Gao-Wald theorem A.0. The Gao-Wald theorem is a case about excited configurations other than the vacuum, and it is saying that, in those cases, there do not even exist bulk geodesics which are as fast as the one on the asymptotic boundary.

Let us then include the end-of-the-world brane Q into consideration. One thing to note is that, while the brane profile is given by $\rho = \rho_*$, the null geodesics, if launching from $\phi = -\pi/2$, also sits on a $\rho =$ const. slice. From this observation, we know that all the null

geodesics on the end-of-the-world brane Q is also a null geodesic in the bulk.

Based on the observations above, let us then check that if statement B, C and D is true for the vacuum configuration shown in figure 7. Thanks to the symmetries we have in this case, it is sufficient to check the following statements respectively. These three statements are taken from statement B.1, C.1, D.1 in our publication [27].

Statement B.1. *Let p be a spacetime point with $p : (\tau, \eta, \rho) = (\tau_p, \eta_p, -\infty)$ and $\mathcal{R}$ be an observer located at $(\eta, \rho) = (\eta_{\mathcal{R}}, -\infty)$ on the asymptotic boundary Σ. Consider sending a signal at the speed of light from p to $\mathcal{R}$. Then $\Delta\tau_\Sigma = \Delta\tau_{\mathcal{M}}$, where $\Delta\tau_\Sigma$ ($\Delta\tau_{\mathcal{M}}$) is the required time on the asymptotic boundary Σ (in the bulk $\mathcal{M}$) for $\mathcal{R}$ to receive the signal.*

Statement C.1. *Let p be a spacetime point with $p : (\tau, \eta, \rho) = (\tau_p, \eta_p, \rho_*)$ and $\mathcal{R}$ be an observer located at $(\eta, \rho) = (\eta_{\mathcal{R}}, \rho_*)$ on the end-of-the-world brane Q. Consider sending a signal at the speed of light from p to $\mathcal{R}$. Then $\Delta\tau_Q = \Delta\tau_{\mathcal{M}}$, where $\Delta\tau_\Sigma$ ($\Delta\tau_{\mathcal{M}}$) is the required time on the brane Q (in the bulk $\mathcal{M}$).*

Statement D.1. *Let p be a spacetime point with $p : (\tau, \eta, \rho) = (\tau_p, \eta_p, \rho_*)$ on the end-of-the-world brane Q and $\mathcal{R}$ be an observer located at $(\eta, \rho) = (\eta_{\mathcal{R}}, -\infty)$ on the asymptotic boundary Σ. Consider sending a signal at the speed of light from p to $\mathcal{R}$. Then $\Delta\tau_{\Sigma\cup Q} > \Delta\tau_{\mathcal{M}}$, where $\Delta\tau_{\Sigma\cup Q}$ ($\Delta\tau_{\mathcal{M}}$) is the required time on $\Sigma \cup Q$ (in the bulk $\mathcal{M}$).*

It is sufficient to consider the following four cases to show these statements. The first case is that both p and $\mathcal{R}$ are on the brane but are not antipodal points. As we have already discussed before, since a geodesic on the brane is also a geodesic in the bulk, there is no bulk shortcut in this case. The second case is that both p and $\mathcal{R}$ are on the asymptotic boundary but are not antipodal points. Similar to the first case, there is no bulk shortcut also in this case. The third case is that p and $\mathcal{R}$ are antipodal points. In this case, one can find infinitely many bulk geodesics which take the same time as the one on Q or Σ, but no one is faster. Combining the above three cases, statement B.1, C.1 and are shown. The fourth case is that p is on the brane and $\mathcal{R}$ is on the asymptotic boundary, but both of them are not on $\partial Q = \partial\Sigma$. In this case, one can always find a bulk geodesic which takes less time than that takes for sending a signal via $Q \cup \Sigma$. This is because the shortest path on $Q \cup \Sigma$ should pass $\partial Q = \partial\Sigma$, which is singular from the bulk point of view. Therefore, a geodesic on the boundary $Q \cup \Sigma$ is no longer a geodesic in the bulk in this case. Therefore, statement D.1 is shown.

Although we have only discussed the AdS_3 case, the extension to general dimensions is straightforward. If we write the metric of a pure AdS_{d+1} as

$$ds^2 = -(r^2+1)d\tau^2 + \frac{dr^2}{r^2+1} + r^2 d\mathbf{\Omega}^2, \tag{5.11}$$

where $d\mathbf{\Omega}^2$ is the line element of S^{d-1}. Comparing this with that in the AdS_3, we can see the only difference is that the S^1 parameterized by ϕ is replaced by S^{d-1}. If we regard all the S^1 structures that appeared in the above discussion as an equator of S^{d-1}, then everything holds in a similar way to the AdS_3 case.

5.4 Causal Structure in AdS/BCFT and Boundary Causality

In this section, we are going to discuss the causal structure in the AdS/BCFT correspondence, and see that this structure is compatible with the causality and locality on the BCFT side. Let us repeat our logic. Since a BCFT is a local quantum field theory, any information propagating happening in this theory should not exceed the speed of light. In other words, one should not be able to send a signal between spacelike separated points on a BCFT. However, in the AdS/BCFT correspondence, this turns out to be a rather nontrivial statement on the bulk gravity side. In fact, since the bottom-up construction of AdS/BCFT [6, 7] is just a bottom-up one, it would not be so surprising even if the bulk dual betrayed our expectation.

The related statement to this topic is statement B. In this case, if we can successfully statement B on the bulk gravity side, then it will provide further support for the bottom-up construction of AdS/BCFT [6, 7].

Since we have already shown statement B in the vacuum configuration in the previous section, now we need to do is to consider the excited configurations. In practice, we would like to show a Gao-Wald-like theorem in the AdS/BCFT case.

As the very first step, we would like to make an assumption about the manifold Σ on which the BCFT is defined. After presenting the statement of the assumption, we will then explain why this assumption is required by the physics associated with BCFT but not a technical one.

The following assumption on Σ is taken from assumption 1 in our publication [27].

Assumption 1. *(Σ, γ_{ij}) can be mapped to $\mathbb{R}^{1,d-2} \times [0,\infty)$ or $\mathbb{R}^{1,d-2} \times [0,l]$ via a Weyl transformation*

$$\gamma_{ij}(x) \to \Omega^2(x)\gamma_{ij}(x), \tag{5.12}$$

where l is a constant.

While this assumption may seem to be too strong, let us explain the reason why it is actually somehow required from the definition of BCFT. For doing so, one thing to emphasize again is the definition of BCFT. While BCFT is a CFT defined on a manifold Σ with boundaries, the inverse is not true. The point is that we require the theory to maximally preserve the conformal symmetry, but not all the Σ are necessarily compatible with that.

Indeed, while 2D BCFT is quite well-studied [8], it is not answered yet what is the most general class of manifolds which are compatible with a BCFT in higher dimensions. In fact, so far, BCFT in higher dimensions are only discussed in $\mathbb{R}^{1,d-2}\times[0,\infty)$ or $\mathbb{R}^{1,d-2}\times[0,l]$. These discussions should be able to be straightforwardly generalized to any manifold satisfying assumption 1 via a conformal transformation. However, for more general shapes of boundaries, it is not clear if one can impose a boundary condition which maximally preserves the conformal symmetries. The Σ itself does not necessarily preserves the conformal symmetries as a manifold after all.

Based on these arguments, we would like to impose the assumption 1 to the manifold Σ we are considering. Although we have introduced this assumption from a physical motivation, we will later see that this assumption plays an important role from a technical point of view.

Let us summarize the statement we would like to show as a theorem.

Theorem B.2. *Let Σ a manifold satisfying assumption 1, and let $\mathcal{M}$ satisfy all the assumptions listed in theorem A.0, then for any two points $p,q\in\Sigma$, if p and q are not causally connected on the asymptotic boundary Σ, then they are not causally connected in the bulk $\mathcal{M}$ either.*

The proof is as follows. The proof here is taken from section 4.2 in our publication [27] with minimal modifications. The modifications are performed to match the notations in this dissertation.

Proof. Consider the asymptotic boundary Σ. The region which can receive a signal through the bulk $\mathcal{M}$ from $p\in\Sigma$ is $A_\Sigma(p,\mathcal{M})$, and the region which can receive a signal through Σ is its causal future $J^+_\Sigma(p)$. To prove theorem B.2, it is sufficient to show

$$\partial A_\Sigma(p,\mathcal{M}) \;\subseteq\; J^+_\Sigma(p). \tag{5.13}$$

Let us firstly see how far we can go without assumption 1. First of all, we can perform an embedding $\Sigma\subset\Sigma'$, $\mathcal{M}\subset\mathcal{M}'$ which satisfy

- $\dim(\Sigma') = \dim(\Sigma)$ and $\dim(\mathcal{M}') = \dim(\mathcal{M})$.
- $\mathcal{M}'$ is a spacetime with a timelike asymptotic boundary $\mathcal{M}' = \Sigma'$.
- $\mathcal{M}'$ satisfies the four conditions given in the Gao-Wald theorem A.0.

Then the Gao-Wald theorem is applicable to $\mathcal{M}'$. A consequence is

$$A_{\Sigma'}(p, \mathcal{M}') \cup \partial A_{\Sigma'}(p, \mathcal{M}') \subseteq J^+_{\Sigma'}(p), \tag{5.14}$$

for any point $p \in \Sigma'$. See [31] for details.

Let us try to derive (5.13) from (5.14). The way of embedding implies

$$A_{\Sigma}(p, \mathcal{M}) \subseteq \left(A_{\Sigma'}(p, \mathcal{M}') \cap \Sigma\right). \tag{5.15}$$

Then we have

$$\begin{aligned}
\partial A_{\Sigma}(p, \mathcal{M}) &\subseteq \left(A_{\Sigma'}(p, \mathcal{M}') \cap \Sigma\right) \ \cup \ \partial\left(A_{\Sigma'}(p, \mathcal{M}') \cap \Sigma\right) \\
&= \left(A_{\Sigma'}(p, \mathcal{M}') \cap \Sigma\right) \ \cup \ \left(\partial A_{\Sigma'}(p, \mathcal{M}') \cap \Sigma\right) \ \cup \ \left(A_{\Sigma'}(p, \mathcal{M}') \cap \partial\Sigma\right) \\
&= \left[A_{\Sigma'}(p, \mathcal{M}') \cap (\Sigma \cup \partial\Sigma)\right] \ \cup \ \left(\partial A_{\Sigma'}(p, \mathcal{M}') \cap \Sigma\right) \\
&= \left(A_{\Sigma'}(p, \mathcal{M}') \cap \Sigma\right) \ \cup \ \left(\partial A_{\Sigma'}(p, \mathcal{M}') \cap \Sigma\right) \\
&= \left(A_{\Sigma'}(p, \mathcal{M}') \cup \partial A_{\Sigma'}(p, \mathcal{M}')\right) \ \cap \ \Sigma \\
&\subseteq \left(J^+_{\Sigma'}(p) \cap \Sigma\right).
\end{aligned} \tag{5.16}$$

Here, we used the property

$$R_1 \subseteq R_2 \quad \Longrightarrow \quad \partial R_1 \subseteq R_2 \cup \partial R_2 \tag{5.17}$$

in the first line, the identity relation

$$\partial(R_1 \cap R_2) = (\partial R_1 \cap R_2) \cup (R_1 \cap \partial R_2) \tag{5.18}$$

in the second line, and

$$(X \cap Z) \cup (Y \cap Z) = (X \cup Y) \cap Z \tag{5.19}$$

in the third line and the fifth line. We also used $\partial\Sigma \subset \Sigma$ in the fourth line and (5.14) in the last line.

Since $J^+_\Sigma(p) \subseteq (J^+_{\Sigma'}(p) \cap \Sigma)$, in order to derive (5.13) from (5.16), we need to show $J^+_\Sigma(p) = (J^+_{\Sigma'}(p) \cap \Sigma)$. However, this does not necessarily hold for general Σ. This is because two points $p, q \in \Sigma$ which can be causally connected through Σ' is not always causally connected through Σ.

So far, we have not used assumption 1 yet. Let us then see how assumption 1 can rescue the situation.

Consider $p, q \in \partial\Sigma$ connected by a null geodesic γ on $\partial\Sigma$, whose tangent vector is given by u. The Gauss-Weingarten equation relates the covariant derivative $\tilde{D}_{\tilde{m}}$ on $\partial\Sigma$ and the covariant derivative D_i on Σ by

$$u^i D_i u^j = (u^{\tilde{m}} \tilde{D}_{\tilde{m}} u^{\tilde{n}}) e^j{}_{\tilde{n}} - k_{\tilde{m}\tilde{n}} u^{\tilde{m}} u^{\tilde{n}} n^j, \tag{5.20}$$

where n^j is the normal vector to $\partial\Sigma$, pointing toward the ambient space. For a geodesic on $\partial\Sigma$

$$u^{\tilde{m}} \tilde{D}_{\tilde{m}} u^{\tilde{n}} = 0 \ , \tag{5.21}$$

and hence

$$u^i D_i u^j = -k_{\tilde{m}\tilde{n}} u^{\tilde{m}} u^{\tilde{n}} n^j. \tag{5.22}$$

This will be a null geodesic in Σ if

$$k_{\tilde{m}\tilde{n}} u^{\tilde{m}} u^{\tilde{n}} = 0 \ . \tag{5.23}$$

Then we will show that (5.23) holds under assumption 1. For $\mathbb{R}^{1,d-2} \times [0, \infty)$ or $\mathbb{R}^{1,d-2} \times [0, l]$, this is trivial. Now consider the Weyl transformation (5.12). Then the extrinsic curvature $k_{\tilde{m}\tilde{n}}$ transforms as

$$k_{\tilde{m}\tilde{n}} \to k'_{\tilde{m}\tilde{n}} = \frac{1}{\Omega} k_{\tilde{m}\tilde{n}} + (n^i \partial_i \Omega) h_{\tilde{m}\tilde{n}} = (n^i \partial_i \Omega) h_{\tilde{m}\tilde{n}} \ . \tag{5.24}$$

Here, $k'_{\tilde{m}\tilde{n}}$ is the extrinsic curvature defined on the manifold after the Weyl transformation and $h_{\tilde{m}\tilde{n}}$ is the induced metric on $\partial\Sigma$. It turns out that the extrinsic curvature is proportional to the induced metric. Therefore, (5.23) holds, i.e. any null geodesic on $\partial\Sigma$ is also a null geodesic on Σ.

Suppose two points $p, q \in \Sigma$ are connected in Σ' by a causal curve $\lambda_{p,q}$ which has an overlap with $\Sigma' \backslash \Sigma$, then there exist $p', q' \in \partial\Sigma$ such that

$$\lambda_{p,q} = \lambda_{p,p'} + \lambda_{p',q'}, + \lambda_{q',q}, \tag{5.25}$$

and

$$\lambda_{p,p'}, \lambda_{q,q'} \in \Sigma. \tag{5.26}$$

Furthermore, there exists a causal curve $\lambda'_{p',q'} \in \partial\Sigma$ which connects p' and q', otherwise, q' would be outside of the light cone of p' and lead to a contradiction with the fact that any null geodesic on $\partial\Sigma$ is also a null geodesic on Σ. In one word, any two points $p, q \in \Sigma$ which are causally connected through Σ' must be causally connected through Σ, and hence

$$J^+_\Sigma(p) = (J^+_{\Sigma'}(p) \cap \Sigma). \tag{5.27}$$

Combining (5.27) with (5.16), we obtain (5.13). Therefore, theorem B.2 is shown.

□

Away from the technical details, let us qualitatively what is nontrivial in this proof, and how assumption 1 plays an important role in it. In one word, the nontrivial point in generalizing the Gao-Wald theorem to AdS/BCFT is that a portion of a larger manifold does not necessarily inherit the causal structure of the original manifold. The most nontrivial events happen at the vicinity of the boundary. The most important consequence of assumption 1 is it implies $k_{\tilde{m}\tilde{n}}u^{\tilde{m}}u^{\tilde{n}} = 0$, which leads to the fact that all null geodesics on $\partial\Sigma$ are also null geodesics on Σ. This feature eventually allows us to embed the causal structure of the current AdS/BCFT setup into a standard AdS/CFT setup which obeys the Gao-Wald theorem.

It would be interesting to note what will happen if we abandon the condition $k_{\tilde{m}\tilde{n}}u^{\tilde{m}}u^{\tilde{n}} = 0$. There are roughly two cases. The first case is that, for any null vector $u^{\tilde{m}}$ on $\partial\Sigma$, $k_{\tilde{m}\tilde{n}}u^{\tilde{m}}u^{\tilde{n}} \leq 0$. In this case, although a null geodesic on $\partial\Sigma$ is not a null geodesic on Σ, the shortest causal path which connects to points on the boundary is a null geodesic on Σ. Therefore, setups in this case are relatively healthy. One may expect a generalization of the Gao-Wald theorem even in this case, but there are more technical details to figure out. The second case is that there exists a null vector $u^{\tilde{m}}$ on $\partial\Sigma$ such that $k_{\tilde{m}\tilde{n}}u^{\tilde{m}}u^{\tilde{n}} > 0$. This case is more severe in the sense that, the shortest causal path which connects two points on $\partial\Sigma$ is in general not even a null geodesic on Σ. It would be interesting to understand what kind of sick behaviors one will observe in such setups.

Let us end this section by commenting on the physical consequences of statement B, which is supported by statement B.1 and theorem B.2. This suggests that one cannot causally connect two spacelike separated points on Σ, which is a necessity for the BCFT defined

on Σ to be a local theory. We have seen that statement B is very nontrivial on the bulk gravity side. In this sense, we have provided further support to the bottom-up AdS/BCFT construction.

5.5 Causal Structure and Nonlocality in the Intermediate Picture

In this section, we consider the causal structure in another bulk-boundary type duality included in the double holography: the Karch-Randall brane-world holography. In other words, we consider the duality between the bulk picture and the intermediate picture. Different from the AdS/BCFT case, now our boundary manifold has two pieces: Q and Σ. Therefore, we need to consider several different cases.

More precisely, we need to first consider the information propagation within the asymptotic boundary Σ. The statement associated with this case is B. Since we have already shown statement B in the previous sections, we can move on to other cases.

The second case to consider is the information propagation within the end-of-the-world brane Q. The statement associated with this case is C. Although we have already checked that this is true for the vacuum configuration, we have not shown it in general cases. Therefore, from now on, we would like to show statement C. We will see that the Neumann boundary condition plays an important role in this case.

The question we would like to ask is if a null geodesic on Q is also a null geodesic in the bulk manifold $\mathcal{M}$. To do so, let us consider an arbitrary curve which lives on Q. Let us denote its tangent vector as u^a. According to the Gauss-Weingarten equation, the covariant derivative D_a defined on the brane Q and the covariant derivative ∇_μ defined in the bulk $\mathcal{M}$ have the following relation:

$$u^\mu \nabla_\mu u^\nu = -K_{ab} u^a u^b n^\nu + (u^a D_a u^c) e^\nu{}_c. \tag{5.28}$$

Here n^ν is the normal vector to the brane Q. Since we are taking the Neumann boundary condition

$$K_{ab} - K h_{ab} - T h_{ab} = 0, \tag{5.29}$$

it is straightforward to find $K_{ab} \propto h_{ab}$. As a result, for a null curve on the brane, we have

$$u^\mu \nabla_\mu u^\nu = (u^a D_a u^c) e^\nu{}_c. \tag{5.30}$$

This implies that, a null geodesic on the brane, and hence by definition $u^a D_a u^b = 0$, is also a null geodesic in the bulk $\mathcal{M}$.

Therefore, one cannot find a causal shortcut in the bulk when sending a signal from a point on the brane to another point on the brane. In other words, we have proven statement C.

It is worth noting that the Neumann boundary condition imposed on the end-of-the-world brane Q is almost the only condition we have used for showing statement C. This is very different from the case of B. Also, note that the Neumann boundary condition also relies on the assumption that there is no localized matter living on the brane. If there are localized matter fields, then the story is slightly different. We will come back and discuss this point later.

The last case we need to consider is to send a signal from Σ to Q or vice versa. This is related to statement D. Although we have only checked this is true in the vacuum case, it is easy to show it in general cases. The point is that, for a general AAdS_{d+1} with an end-of-the-world brane, its asymptotic structure is the same as that of the vacuum configuration. On the other hand, the existence of causal shortcuts in this case comes from the singular behavior occurring at the intersection between the end-of-the-world-brane Q and the asymptotic boundary Σ. Therefore, the same statement should also be true for general configurations as long as the asymptotic structure is unchanged.

Now we have shown all the statements B, C and D. If we consider the Karch-Randall brane-world holography, the boundary theory is the intermediate picture of double holography defined on $\Sigma \cup Q$. From the three statements we have shown, perhaps the most important feature of the effective theory in the intermediate picture is that, it must include effective superluminal information propagation when considering sending a signal from Σ to Q or vice versa. This is because there always exist two points which are spacelike separated on $\Sigma \cup Q$ but causally connected in the bulk $\mathcal{M}$. In fact, one can also explicitly confirm that the commutator between local fields defined on two spacelike separated points on $\Sigma \cup Q$ can be nonvanishing from holographic computation (See section 6 of [27].). Since a local theory with local Poincaré symmetry cannot contain superluminal effects, and the current intermediate picture does not seem to break the local Poincaré symmetry, the effective theory defined on $\Sigma \cup Q$ is expected to be nonlocal.

As we have reviewed in the introduction part, since the intermediate picture is expected

to reflect the quantum nature of gravity, we would like to understand this nonlocality as a property of quantum gravity.

From this point of view, the next question to ask is how one can get a nonlocal effective theory from a local gravitational action when taking the quantum effects into consideration. The phenomenon we observed might be natural if one considers the path integral formalism of quantum gravity. In the path integral formalism, one needs to sum over all possible geometries with a given boundary condition. Therefore, one needs to consider a superposition over different geometries. As a result, if one would like to approximate the whole path integral as an effective theory on the most dominating geometry, then the fluctuation of the geometry may appear as a nonlocal term. This phenomenon is in fact not strange since there exist known examples. One famous example is a $T\bar{T}$-deformed CFT. It is known that a $T\bar{T}$-deformed CFT can be written as a sum over random geometries or as a nonlocal theory defined on a fixed geometry [61]. In the double holography case, a more precise question is how one can derive effective nonlocal action using gravitational path integrals. It is worth noting that one can observe similar effects in the canonical formalism of quantum gravity [62].

5.6 Comments on Causal Structures in Other Holographic Setups

Till now, we have discussed the causal structure in double holography. We have found that the causal structure in the bulk picture is compatible with causality and locality in the BCFT picture, by considering AdS/BCFT as a bulk-boundary type duality. On the other hand, for the Karch-Randall holography to be compatible with the bulk causal structure, there must exist effective superluminal phenomena in the intermediate picture, i.e. the boundary theory of the Karch-Randall brane-world holography.

In the procedure of proving statements B, C, D, we find that there are various mechanisms which are crucial to determining the causal structures.

First of all, if one wants to show that two spacelike separated points on the asymptotic boundary are also spacelike separated in the bulk gravity, one needs to use a Gao-Wald-like argument, which requires ANEC and other conditions in the bulk gravity.

On the other hand, if one pushes the manifold on which a "boundary theory" is defined into the bulk from the asymptotic boundary, since the Gao-Wald-like argument will be broken, two spacelike separated points on this manifold can in general be causally connected in the bulk.

However, if the boundary manifold is an end-of-the-world brane, then the bulk shortcuts are magically avoided thanks to the Neumann boundary condition imposed on the brane. With the Neumann boundary condition on the brane, one can show that a null geodesic on the brane must also be a null geodesic in the bulk. Therefore, two spacelike points on the brane are not causally connected in the bulk. It is somehow surprising that this argument does not put requirements such as ANEC on the bulk gravity side.

In a bulk-boundary type duality, once two spacelike separated points on the boundary side can be causally connected in the bulk, then the effective theory defined on the boundary side must be nonlocal.

Based on the above observations, let us comment on the causal structures and locality in some other holographic correspondences.

5.6.1 $T\bar{T}$-deformed CFT/cutoff AdS correspondence

As the very first example, let us consider the holography associated with the $T\bar{T}$-deformed CFT [61,63,64]. It is known that the holographic dual of such a theory is an AdS gravity with a finite radial cutoff. Different from the standard AdS/CFT correspondence, the boundary theory does not live on the asymptotic boundary, but on the finite cutoff surface [65].

As we have explained above, once one pushes the manifold on which the boundary is defined into the bulk from the asymptotic boundary, the Gao-Wald theorem does not work anymore, and one in general can find causal shortcuts in the bulk.

Indeed, people have found explicit causal shortcuts [65–67] in previous research. This then implies the boundary theory in this holographic correspondence should be nonlocal, and indeed it is already known that the $T\bar{T}$-deformed theory is nonlocal [61]. In fact, one can even confirm that the effective information propagation speed on the two sides is equal in this correspondence [65]. In this sense, $T\bar{T}$-deformed CFT/cutoff AdS correspondence serves as a perfect example which reflects the spirit explained at the beginning of this section.

5.6.2 Randall-Sundrum brane-world holography

In this dissertation, we mainly consider the end-of-the-world branes with tension $-(d-1)/L < T < (d-1)/L$. In this regime, the brane intersects the asymptotic boundary in a timelike way, and the brane itself describes an AdS universe. As we have already introduced, this is called the Karch-Randall brane-world holography.

On the other hand, there is also the Randall-Sundrum brane-world holography [33, 34] where the brane tension is $|T| \geq (d-1)/L$. More precisely, $|T| = (d-1)/L$ describes flat branes and $|T| > (d-1)/L$ describes dS branes. These kinds of brane-world models are widely studied from phenomenological motivation.

One may wonder causal structures in the Randall-Sundrum brane-world holography. In fact, if there is no localized matter on the branes, then although the tension of the brane is different from the Karch-Randall case, the boundary condition imposed on the brane is the same Neumann-type boundary condition. As a result, one will find similar results to that we found in the KR case, i.e. two spacelike separated points on the dS/flat brane-world are also spacelike separated in the bulk, and there is no bulk shortcut [68].

5.6.3 Brane-worlds with localized matter

As the last example, let us consider brane-worlds with localized matter on it. We will still take the Neumann boundary condition, but in this case the boundary condition is modified by the existence of the matter field:

$$K_{ab} - Kh_{ab} - Th_{ab} + 8\pi G_N T^Q_{ab} = 0 \ , \tag{5.31}$$

where T^Q_{ab} is the (localized) matter stress-energy tensor on the brane. From this boundary condition, we can immediately find

$$K_{ab} = -\frac{1}{d-1} T h_{ab} - 8\pi G_N \left(T^Q_{ab} - \frac{T^Q}{d-1} h_{ab} \right) . \tag{5.32}$$

If the NEC

$$T^Q_{ab} u^a u^b \geq 0 \ . \tag{5.33}$$

is imposed on the brane, we will get

$$K_{ab} u^a u^b = -8\pi G_N T^Q_{ab} u^a u^b \leq 0 \ , \tag{5.34}$$

which implies that the brane is concave in the null direction. In this case, null geodesics in the bulk connect spacelike separated points on the brane. Application of this statement to cosmology is discussed in [68].

6 Pseudo Entropy and its Application

In this chapter, we present a generalization of entanglement entropy to the post-selection setups. Before doing that, we would like to introduce the original motivation why we would like to introduce it by asking a simple question in AdS/CFT. We will then present its basic properties and some of its applications to quantum many-body systems. This chapter is based on a part of [21, 23, 26].

6.1 More General Minimal Surfaces in AdS/CFT

In section 2.4, we have explained how to compute the entanglement entropy in a holographic CFT using its gravity dual, when the setup is static. In general, this prescription can be applied when the setup is Euclidean time reflection symmetric. It turns out that the entanglement entropy can be computed via the RT formula from a class of minimal surfaces in the gravity dual, which are codimension-two, anchor on the asymptotic boundary, and sit in a Euclidean time reflection symmetric slice.

These minimal surfaces which give the entanglement entropy are in a very special class. From the point of view of the AdS side, we would like to understand what are the corresponding quantities for more general surfaces on the CFT side. To this end, let us first consider the most simple generalization: we consider codimension-two surfaces that anchor on the asymptotic boundary but do not necessarily sit in a Euclidean time reflection symmetric slice. In other words, we would like to consider Euclidean setups where the time reflection symmetry is broken.

In the language of Euclidean path integral, the time reflection symmetry plays an important role in the sense that it guarantees the two sides of the time slice give the bra and the ket for the same state. Therefore, when computing correlation functions on this time slice, one can get the expectation value for this state.

On the other hand, if we consider a time slice without Euclidean time reflection symmetry, we will be considering the case where the bra and the ket are in general different. Therefore, we would like to introduce an entropy-like quantity associated with such a setup to answer our original question. This leads to the introduction of pseudo entropy in the following.

6.2 Definition and Basic Properties of Pseudo Entropy

Before defining the pseudo entropy, let us firstly define transition matrices from two pure states. For two pure quantum states $|\psi\rangle$ and $|\varphi\rangle$ that are not orthogonal to each other, we can consider the following normalized matrix

$$\mathcal{T}^{\psi|\varphi} \equiv \frac{|\psi\rangle\langle\varphi|}{\langle\varphi|\psi\rangle}. \tag{6.1}$$

This matrix corresponds to a post-selection experiment [69] where one prepares an initial state $|\psi\rangle$, performs some operations on it, and then post-selects the final state to $|\varphi\rangle$. We call $\mathcal{T}^{\psi|\varphi}$ a transition matrix.

Then let us consider dividing the whole system into A and B. Accordingly, the Hilbert space will be able to be written as $\mathcal{H} = \mathcal{H}_A \otimes \mathcal{H}_B$. It is then straightforward to introduce the reduced transition matrix as $\mathcal{T}_A^{\psi|\varphi} \equiv \mathrm{Tr}_B\left[\mathcal{T}^{\psi|\varphi}\right]$.

Let us work on the reduced transition matrix. We can introduce a Rényi entropy-like quantity as

$$S^{(n)}(\mathcal{T}_A^{\psi|\varphi}) \equiv \frac{\log \mathrm{Tr}\left[(\mathcal{T}_A^{\psi|\varphi})^n\right]}{1-n}, \tag{6.2}$$

where n is an integer greater than 1.

Taking the $n \to 1$ limit, one will get a von Neumann entropy-like quantity given by

$$S(\mathcal{T}_A^{\psi|\varphi}) = -\mathrm{Tr}\left(\mathcal{T}_A^{\psi|\varphi} \log \mathcal{T}_A^{\psi|\varphi}\right). \tag{6.3}$$

There are several subtle points in this definition, but we would like to omit the discussion since we will not encounter those subtle points throughout this dissertation. One can see appendix A in [21] for more details.

Note that since a transition matrix is in general not Hermitian, its eigenvalues are not necessarily real. Therefore, the pseudo entropy is in general complex. Besides, although we defined the pseudo entropy as an entropy-like quantity, we cannot call it entropy because it does not satisfy all the axioms required for an entropy such as convexity. In fact, this is the reason why we call it pseudo entropy.

Let us then move on to see some basic properties of pseudo (Rényi) entropy. It is easy to prove the following basic properties for $n \in \mathbb{R}^+$.

First of all, if $|\psi\rangle$ is a product state with respect to $\mathcal{H}=\mathcal{H}_A\otimes\mathcal{H}_B$, then the pseudo Rényi entropy is zero, i.e. $S^{(n)}(\mathcal{T}_A^{\psi|\varphi})=0$. The is because when $|\psi\rangle=|\psi'\rangle_A|\psi''\rangle_B$, one can find $\left(\mathcal{T}_A^{\psi|\varphi}\right)^n=\mathcal{T}_A^{\psi|\varphi}$.

Second, if $\mathrm{Tr}(\mathcal{T}_A^{\psi|\varphi})^n$ and all eigenvalues of $\mathcal{T}_A^{\psi|\varphi}$ are in $\mathbb{C}\backslash\mathbb{R}^-$, then $S^{(n)}(\mathcal{T}_A^{\psi|\varphi})=S^{(n)}(\mathcal{T}_A^{\varphi|\psi})^*$. This follows directly from the relation $\mathcal{T}^{\psi|\varphi}=\left[\mathcal{T}^{\varphi|\psi}\right]^\dagger$.

Finally, one can easily find that the pseudo (Rényi) entropy is symmetric with respect to bipartitions, i.e. $S^{(n)}(\mathcal{T}_A^{\psi|\varphi})=S^{(n)}(\mathcal{T}_B^{\psi|\varphi})$.

6.3 Pseudo Entropy in Ising Model

As an application of the pseudo entropy, we would like to show a relation between pseudo entropy and quantum phase transitions in quantum many-body systems. As a concrete example, let us consider a transverse Ising spin chain model. More precisely, let us consider one with N spins labeled by $j=0,1,\cdots,N-1$ and the periodic boundary condition. The Hamiltonian of such a model is given by

$$H=-J\sum_{j=0}^{N-1}\sigma_j^z\sigma_{j+1}^z-h\sum_{j=0}^{N-1}\sigma_j^x, \tag{6.4}$$

Here σ_i^z is the Pauli operator associated with the i-th spin. We take the convention where the eigenvalues of the Pauli operators are ±1.

Let us consider the ground state of such an Ising spin chain. Let us denote the ground state as $|\Omega_{(J,h)}\rangle$. By changing the parameters (J,h), we can realize a class of ground states, and there is a quantum phase transition happening here [70]. More precisely, noting that the ratio J/h is the only physical freedom, the quantum critical point sits at $J=h$. $J>h$ is the ferromagnetic phase. On the other hand, $J<h$ is the paramagnetic phase.

Let us pick up two sets of (J,h) and denote them as (J_1,h_1) and (J_2,h_2), respectively. We consider the transition matrix defined as

$$\mathcal{T}^{1|2}=\frac{|\Omega_{(J_1,h_1)}\rangle\langle\Omega_{(J_2,h_2)}|}{\langle\Omega_{(J_2,h_2)}|\Omega_{(J_1,h_1)}\rangle}. \tag{6.5}$$

Besides, let us denote $\rho_1=|\Omega_{(J_1,h_1)}\rangle\langle\Omega_{(J_1,h_1)}|$ and $\rho_2=|\Omega_{(J_2,h_2)}\rangle\langle\Omega_{(J_2,h_2)}|$. Divide the spin chain into two parts, pick up A as a single interval with N_A spins, and consider the entanglement entropy and pseudo entropy associated with A. Some numerical results are shown below. Note that the python package quspin [71] was used in our computation.

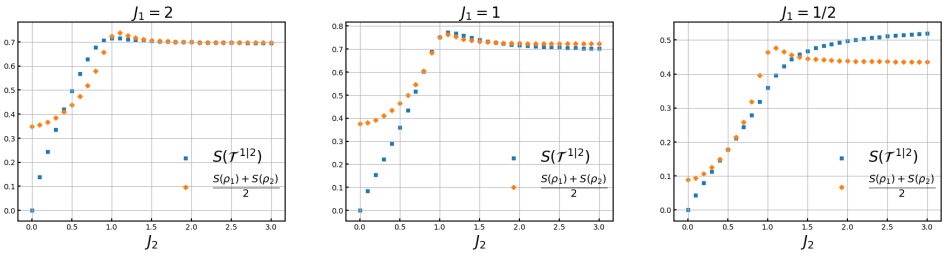

Figure 9: Pseudo entropy (blue) and averaged entanglement entropy (orange) for a single interval A. Here, the total spin number is $N = 16$, the interval length is $N_A = 8$. Also, we normalize the parameter h as $h_1 = h_2 = 1$. We set $J_1 = 2$ (left), $J_1 = 1$ (middle) and $J_1 = 1/2$ (right). The value of J_2 is shown in the horizontal axis. The plots are taken from figure 5 in our publication [23].

There are two key observations in the numerical results. The first one is that the difference $\Delta S_{12} = S(\tau_A^{1|2}) - \frac{S(\rho_A^1)+S(\rho_A^2)}{2}$ is always negative, i.e. $\Delta S_{12} \leq 0$ when the two ground states $|\Omega_{J_1,h_1}\rangle$ and $|\Omega_{J_2,h_2}\rangle$ are in the same phase. The second observation is that the difference ΔS_{12} can be positive if $|\Omega_{J_1,h_1}\rangle$ and $|\Omega_{J_2,h_2}\rangle$ are in different phases. Therefore, from these two observations, one may expect that the pseudo entropy can serve as an order parameter for distinguishing two different phases.

In fact, although we have only shown the transverse Ising model as an example, we have also confirmed that the same phenomenon also happens in the quantum XY model which has a much richer phase structure. See [26] for more details.

7 Spacelike Boundaries, dS Branes and Holography

Till now, we have mainly worked in variations of BCFT in Lorentzian signatures with timelike boundaries, as well as gravity duals associated with them. On the other hand, Lorentzian CFT with spacelike boundaries are hardly ever discussed in the literature. There are two reasons with respect to this point.

The first one is that field theories with spacelike boundaries are hard to analyze. For example, BCFTs are originally formulated as Euclidean theories, and by analytic continuation of the Euclidean time to a real time, one can easily get BCFTs with timelike boundaries. However, BCFT[1] with spacelike boundaries cannot be obtained in this way.

The second reason is that we usually do not have sufficient motivation to consider BCFT with spacelike boundaries. In most cases when we use path integral to discuss quantum systems, our purposes are usually to get some information about a specific (possibly mixed) state. However, when introducing a spacelike boundary or more in a Lorentzian setup, the path integral will in general no more simulate a density matrix but a transition matrix. To see this point, let us take a QFT defined on a half of $\mathbb{R}^{1,1}$ parameterized by (t, x) where $t \in [0, \infty)$ and $x \in (-\infty, \infty)$. Let us denote the boundary state we impose at $t = 0$ as $|B\rangle$. If we take the time slice $t = t_0$, then the ket realized on it by the path integral over $0 < t < t_0$ is $e^{-iHt_0} |B\rangle$, where H is the Hamiltonian, and the bra realized on it by the path integral over $t_0 < t$ is the ground state $\langle 0|$.

In this chapter, we will see that BCFT with spacelike boundaries can be straightforwardly realized by slightly generalizing the gravity setup of AdS/BCFT. Due to the nature that a BCFT with spacelike boundaries realizes a transition matrix but not a density matrix, entropy-like quantities computed in these setups should be interpreted as pseudo entropy but not entanglement entropy. We will also discuss this point in specific models. This chapter is based on a part of our publications [22].

7.1 Generalizing AdS/BCFT

To begin with, let us consider a BCFT defined on a Euclidean disk with radius r. Let us use $(w, \bar{w})$ to parameterize the BCFT. Then the disk is given by $w\bar{w} \leq r^2$. By solving the

[1]It is not necessarily proper to call a CFT defined on a manifold with spacelike boundaries a BCFT. However, we would like to just call them BCFT in the following with a little bit abuse of terminology.

equation of motion, it is straightforward to find that the metric in its gravity dual is given by the Poincaré metric

$$ds^2 = \frac{dwd\bar{w} + dz^2}{z^2} \tag{7.1}$$

and the brane profile is given by

$$w\bar{w} + (z - r\text{sinh}[\text{arctanh}(T)])^2 = (r\text{cosh}[\text{arctanh}(T)])^2 \tag{7.2}$$

where T is the brane tension. For simplicity, we fixed the AdS radius L to be 1.

Let us introduce a new set of parameters such that

$$T = \frac{\alpha}{\beta}, \tag{7.3}$$

$$r^2 = \beta^2 - \alpha^2, \tag{7.4}$$

then the brane profile can be rewritten as

$$w\bar{w} + (z - \alpha)^2 = \beta^2. \tag{7.5}$$

It is straightforward to see that the intersection between the brane profile and the asymptotic boundary is

$$w\bar{w} = \beta^2 - \alpha^2 = r^2. \tag{7.6}$$

If we regard $w \equiv x + i\tau$ and perform the analytic continuation $\tau = it$, then the boundary of the BCFT turns into

$$x^2 - t^2 = \beta^2 - \alpha^2 > 0, \tag{7.7}$$

which is timelike in the Lorenzian setup.

This is a standard AdS/BCFT setup where $-1 < T < 1$. Then a natural question to ask is what if we consider the case where $|T| > 1$. In this case, in the Lorentzian setup, the brane will intersect the asymptotic boundary at

$$x^2 - t^2 = \beta^2 - \alpha^2 < 0, \tag{7.8}$$

which turns out to be spacelike. If we go back to the Euclidean setup, one will find that the brane Q floats in the bulk and does not intersects the asymptotic boundary. In this sense, the

CFT description stays to be mysterious. However, we can apply the gravity dual to analyze the BCFT with spacelike boundaries!

Moreover, the brane Q turns out to be dS but not AdS in this case [72], which suggests that the current setup should be useful to study dS holography. This provides us a strong motivation to investigate such setups.

7.2 Holographic Pseudo Entropy

In this section, let us compute the pseudo entropy associated with the holographic BCFT with spacelike boundaries introduced in the previous section.

To be concrete and for simplicity, let us consider a half-infinite subsystem $A = [a, \infty)$ with just one endpoint at $x = a$. Similar to the holographic entanglement entropy case, the holographic pseudo entropy in this setup can be evaluated as

$$S_A = \frac{\text{Area}(\Gamma_A)}{4G_N}, \tag{7.9}$$

in the corresponding Euclidean setup. Here, Γ_A is a geodesic which connects $(\tau, x, z) = (\tau, a, \epsilon)$ and the end-of-the-world brane Q. There are many such geodesics, but we take the one with the shortest length as Γ_A.

Let us consider the case where the end-of-the-world brane looks like a bubble, and the physical region is taken as the outside of the bubble:

$$x^2 + \tau^2 + (z - \alpha)^2 \geq \beta^2. \tag{7.10}$$

See figure 10 for a sketch. Accordingly, what we need to do is to find out and evaluate the shortest geodesic which connects $(\tau, x, z) = (\tau, a, \epsilon)$ and the brane Q.

Thanks to the rotational symmetry of the current setup, we can consider a simple case where $\tau = 0$ without loss of generality. In this case, considering the reflection symmetry with respect to $\tau = 0$, the minimal geodesic Γ_A should lie in the $\tau = 0$ slice.

First of all, for an arbitrary point $(\tau, x, z) = (0, \xi, \zeta)$, note that the distance between $(\tau, x, z) = (0, a, \epsilon), (0, \xi, \zeta)$ is given by

$$\cosh^{-1}\left(\frac{(a-\xi)^2 + \zeta^2 + \epsilon^2}{2\epsilon\zeta}\right) \simeq \log\left(\frac{(a-\xi)^2 + \zeta^2}{\epsilon\zeta}\right). \tag{7.11}$$

Since we would like to look for the minimal geodesic which ends on $x^2 + \tau^2 + (z - \alpha^2) = \beta^2$, we would like to restrict $(\tau, x, z) = (0, \xi, \zeta)$ on it. In this case, it is straightforward to find

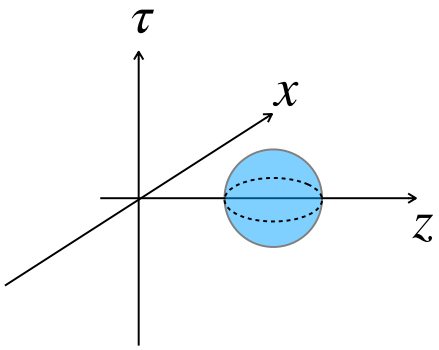

Figure 10: A sketch of the Euclidean counterpart of the gravity dual of a BCFT with spacelike boundaries. The end-of-the-world brane Q is shown in blue. The physical region is that outside of the bubble Q. On the other hand, the region inside the bubble is excluded.

that

$$\text{Area}(\Gamma_A) = \log\left(\frac{a^2+\alpha^2-\beta^2}{(\alpha+\beta)\epsilon}\right), \tag{7.12}$$

which is realized at

$$\xi = \frac{2a\beta(\alpha+\beta)}{a^2+(\alpha+\beta)^2}, \tag{7.13}$$

$$\zeta = \frac{(\alpha+\beta)(a^2+\alpha^2-\beta^2)}{a^2+(\alpha+\beta)^2}. \tag{7.14}$$

Considering the rotation symmetry of the current setup, if we set the edge of the subsystem A at $(\tau, x, z) = (\tau, a, \epsilon)$, then we can find,

$$\text{Area}(\Gamma_A) = \log\left(\frac{\tau^2+a^2+\alpha^2-\beta^2}{(\alpha+\beta)\epsilon}\right). \tag{7.15}$$

Accordingly, the holographic pseudo entropy is evaluated as

$$S_A = \left.\frac{\text{Area}(\Gamma_A)}{4G_N}\right|_{\tau=it} = \frac{c}{6}\log\left(\frac{-t^2+a^2+\alpha^2-\beta^2}{(\alpha+\beta)\epsilon}\right). \tag{7.16}$$

In this way, we have not only extended BCFT to those with spacelike boundaries, but also succeeded to evaluate its holographic pseudo entropy using the holographic dual. See [24] for more analyses on BCFT setups with spacelike boundaries, the evaluation of holographic pseudo entropy and their relations with the black hole singularity.

8 Conclusion and Future Directions

In this dissertation, we presented various developments of AdS/BCFT and quantum information related to holography. After reviewing the general backgrounds, we started by discussing generalizations of BCFT and their gravity duals with time like boundaries. The first is the moving mirror setups where the boundaries have a time-independent trajectory in chapter 3. We presented a conformal map method which relates complicated moving mirror setups to simple ones in CFT. We also explained how moving mirror setups can be related to realistic evaporating black holes in dynamical gravity using the language of double holography. After that, we move on to another setup arising from AdS/BCFT with timelike boundaries called the wedge holography in chapter 4. The wedge holography is constructed by introducing two end-of-the-world branes which are parallel to each other on the bulk side. This causes a dimensional reduction on the boundary side, which brings the original BCFT_d to a CFT_{d-1}. We also presented holographic computations of CFT quantities from the bulk gravity side. In chapter 5, we discussed an important feature in Lorentzian setups, the causal structure. Focusing on the two bulk-boundary-type dualities in the double holography, we first showed that the causal structure in the bulk picture is compatible with causality and locality in the BCFT picture. This is a generalization of the Gao-Wald theorem [31] with the presence of boundaries, and provides further support to the bottom-up AdS/BCFT construction. Then we pointed out that the causal structure in the bulk picture implies that there exist intrinsic superluminal effects in the intermediate picture in Karch-Randall brane-world holography. In chapter 6, we introduced a new quantum informational quantity called pseudo entropy with a motivation coming from holography. We then saw that pseudo entropy is useful even outside of the holography context. As a concrete example, we showed its usefulness for distinguishing different quantum phases. In chapter 7, we first explained why field theories with spacelike boundaries are difficult to analyze and usually considered to be less interesting. We then showed that BCFT with spacelike boundaries can be easily realized on the gravity side of the AdS/BCFT correspondence. Furthermore, such setups can be related to dS brane-worlds via double holography, which gives us a strong motivation to study them. We showed a simple concrete construction and computed the pseudo entropy associated with the setup.

There are many intriguing future directions for the topics discussed in this dissertation. We will discuss some of them in the following.

Conformal Bootstrap and AdS/BCFT

In this dissertation, we have seen that double holography plays an important role in the study of quantum gravity recently. Double holography has three equivalent pictures: the bulk picture which is often taken to the semiclassical limit, the BCFT picture, and the intermediate picture which reflects many features of quantum gravity. However, the only UV-complete picture is the BCFT picture. Therefore, it is expected that studying the BCFT picture will lead us to a deeper understanding of quantum gravity. The conformal bootstrap is a powerful method to study conformal field theories. Conformal field theories have a lot of symmetries that allow one to fix many quantities with a small number of inputs using self-consistency conditions. This is called the conformal bootstrap. Obviously, the conformal bootstrap is also a powerful method in BCFT. Therefore, it is natural to expect that using conformal bootstrap to study AdS/BCFT will be useful to study quantum gravity.

There is another more straightforward but important motivation to study the conformal bootstrap in AdS/BCFT. In AdS/BCFT, because of the existence of the end-of-the-world branes in the bulk, the gravity side becomes more complicated compared to standard AdS/CFT. In the semiclassical limit, the gravity dual of the field theory is the solution of the Einstein equation which minimizes the gravitational action. While finding a solution to the Einstein equation may be not so hard, it is in general nontrivial to judge if the found solution is the minimal one. Therefore, one may make a mistake to identify a fake solution as the gravity dual of a given BCFT, which can lead to various mysterious observations. On the other hand, there is no such ambiguity on the BCFT side. Therefore, bootstrapping on the BCFT side can also help us avoid confusion on the gravity side.

A bootstrap program in AdS/BCFT has been initiated by us in [51]. In [51], we apply the conformal bootstrap on the BCFT side to several mysterious points in AdS/BCFT. For example, we show that self-intersections [73, 74] of the end-of-the-world brane do not happen on the gravity side in $AdS_3/BCFT_2$. We have already obtained many important results by solving the most basic bootstrap equation. It is expected that one will get more useful information by solving other bootstrap equations.

Causality and Brane-world Holography

One result we discussed in section 5 is that the intermediate picture should include an intrinsic superluminal effect in order to be compatible with the causal structure in the bulk picture. There are two ways to understand this result, depending on whether one considers

this superluminal effect as physical or not.

The reason that one may take the first stance is that the intermediate picture is known to capture quantum features of gravity such as the island structures [10]. In this case, we need to understand in which sense one may observe a superluminal effect in quantum gravity. We note that observing an effective superluminal signal does not mean the underlying UV theory breaks causality. In fact, there always exists ambiguity to define the background geometry and locality in a quantum theory of gravity [75]. From this stance, it would be important to understand how to derive effective superluminal propagation in formulations other than holography.

The reason that one may take the second stance is that the Karch-Randall brane-world holography is after all a bottom-up model. Therefore, we should not expect everything to go right in it. An important development that takes this stance is [76]. In [76], the authors constructed a top-down model of double holography. In particular, they constructed not only a bulk picture but also an intermediate picture for a common BCFT, which comprises 4D $\mathcal{N} = 4$ super Yang-Mills on a half space coupled to a 3D super symmetric CFT on its boundary. In its bulk dual, the spacetime can be divided into an AdS_5 region and an AdS_4 region. They found that if one naively regards the AdS_4 region as the gravitational region one would find in an intermediate picture, then one again finds causal shortcuts in the bulk, as we observed in the bottom-up setups. On the other hand, their intermediate picture is constructed by firstly dividing the $BCFT_4$ into an $SCFT_3$ and the other part artificially, then applying AdS_4/CFT_3 to the $SCFT_3$ part. They argued that the intermediate picture they constructed does not contain any superluminal effects by construction. However, they pointed out that the AdS_4 geometry they obtained in their intermediate picture does not match the AdS_4 geometry in their bulk picture, which may suggest that the Karch-Randall holography is not exact. From this stance, we need to understand to what extent the Karch-Randall holography is true. Some features of Karch-Randall holography, such as the massive nature of graviton [9,41], will not be changed even if it is not exact. On the other hand, there are also many arguments and results which heavily rely on the exact matching of the brane geometries on the two sides (see e.g. [77–79]). However, one thing important to point out is that one should be able to construct different kinds of intermediate pictures, and the one constructed in [76] is just one specific example. It would also be interesting to understand the relation between different intermediate pictures.

dS Holography and Quantum Measurement

In section 7, we have seen that considering an analytic continuation on the bulk gravity side of AdS/BCFT not only gives a straightforward way to realize BCFT with spacelike boundaries but also gives us a strong motivation to study such setups. While it is still not clear how to extract information on the dS branes in such setups, we expect that they will provide useful hints.

Another important physical meaning associated with spacelike boundaries that we did not explicitly discuss in the main text is spacelike boundaries realize the most simple type of quantum measurements, the forced measurements. While measurement is one of the most important ingredients in quantum theory, it is hardly ever explicitly discussed in quantum field theories and quantum gravity, partially because it is difficult to treat in these systems. On the other hand, in recent years, people have started to introduce the effect of measurements into quantum many-body systems and found many interesting structures [80–82]. Therefore, it would be intriguing to study the relation between measurements and BCFTs with spacelike boundaries, though these setups are extremely simple. Through AdS/BCFT, these may also give us hints on how to treat measurements in quantum gravity.

Acknowledgements

I am deeply grateful to my supervisor, Tadashi Takayanagi. Tadashi has opened the door and led me to the world of theoretical physics. I am always fascinated by the way how Tadashi thinks about the world and by his discernment about the deepest part behind a phenomenon. Thanks to his edification, I could gradually shape my own point of view.

I also would like to thank my other collaborators, including Ibra Akal, Pawel Caputa, Taishi Kawamoto, Yuya Kusuki, Ali Mollabashi, Yoshifumi Nakata, Tokiro Numasawa, Hidetoshi Omiya, Shan-Ming Ruan, Noburo Shiba, Teppei Shimaji, Kotaro Tamaoka, Yusuke Taki and Yasushi Yoneta. They supported and taught me a lot during our collaborations.

My work was supported by Grant-in-Aid for JSPS Fellows No. 20J23116, by the ANRI Fellowship, and by a Graduate Fellowship from the Kavli Institute for Theoretical Physics, University of California, Santa Barbara.

References

[1] G. 't Hooft, *Dimensional reduction in quantum gravity*, *Conf. Proc.* **C930308** (1993) 284 [gr-qc/9310026].

[2] L. Susskind, *The World as a hologram*, *J. Math. Phys.* **36** (1995) 6377 [hep-th/9409089].

[3] J. M. Maldacena, *The Large N limit of superconformal field theories and supergravity*, *Adv. Theor. Math. Phys.* **2** (1998) 231 [hep-th/9711200].

[4] A. Strominger, *The dS / CFT correspondence*, *JHEP* **10** (2001) 034 [hep-th/0106113].

[5] M. Alishahiha, A. Karch, E. Silverstein and D. Tong, *The dS/dS correspondence*, *AIP Conf. Proc.* **743** (2004) 393 [hep-th/0407125].

[6] T. Takayanagi, *Holographic Dual of BCFT*, *Phys. Rev. Lett.* **107** (2011) 101602 [1105.5165].

[7] M. Fujita, T. Takayanagi and E. Tonni, *Aspects of AdS/BCFT*, *JHEP* **11** (2011) 043 [1108.5152].

[8] J. L. Cardy, *Boundary conformal field theory*, hep-th/0411189.

[9] A. Karch and L. Randall, *Locally localized gravity*, *JHEP* **05** (2001) 008 [hep-th/0011156].

[10] A. Almheiri, R. Mahajan, J. Maldacena and Y. Zhao, *The Page curve of Hawking radiation from semiclassical geometry*, *JHEP* **03** (2020) 149 [1908.10996].

[11] S. W. Hawking, *Particle Creation by Black Holes*, *Commun. Math. Phys.* **43** (1975) 199.

[12] S. W. Hawking, *Particle Creation by Black Holes*, *Commun. Math. Phys.* **43** (1975) 199.

[13] D. N. Page, *Information in black hole radiation*, *Phys. Rev. Lett.* **71** (1993) 3743 [hep-th/9306083].

[14] A. Almheiri, N. Engelhardt, D. Marolf and H. Maxfield, *The entropy of bulk quantum fields and the entanglement wedge of an evaporating black hole*, *JHEP* **12** (2019) 063 [1905.08762].

[15] G. Penington, *Entanglement Wedge Reconstruction and the Information Paradox*, *JHEP* **09** (2020) 002 [1905.08255].

[16] A. Almheiri, T. Hartman, J. Maldacena, E. Shaghoulian and A. Tajdini, *Replica Wormholes and the Entropy of Hawking Radiation*, *JHEP* **05** (2020) 013 [1911.12333].

[17] G. Penington, S. H. Shenker, D. Stanford and Z. Yang, *Replica wormholes and the black hole interior*, 1911.11977.

[18] A. Almheiri, T. Hartman, J. Maldacena, E. Shaghoulian and A. Tajdini, *The entropy of Hawking radiation*, 2006.06872.

[19] S. Ryu and T. Takayanagi, *Holographic derivation of entanglement entropy from AdS/CFT*, *Phys. Rev. Lett.* **96** (2006) 181602 [hep-th/0603001].

[20] S. Ryu and T. Takayanagi, *Aspects of Holographic Entanglement Entropy*, *JHEP* **08** (2006) 045 [hep-th/0605073].

[21] Y. Nakata, T. Takayanagi, Y. Taki, K. Tamaoka and Z. Wei, *New holographic generalization of entanglement entropy*, *Phys. Rev. D* **103** (2021) 026005 [2005.13801].

[22] I. Akal, Y. Kusuki, T. Takayanagi and Z. Wei, *Codimension two holography for wedges*, *Phys. Rev. D* **102** (2020) 126007 [2007.06800].

[23] A. Mollabashi, N. Shiba, T. Takayanagi, K. Tamaoka and Z. Wei, *Pseudo Entropy in Free Quantum Field Theories*, *Phys. Rev. Lett.* **126** (2021) 081601 [2011.09648].

[24] I. Akal, Y. Kusuki, N. Shiba, T. Takayanagi and Z. Wei, *Entanglement Entropy in a Holographic Moving Mirror and the Page Curve*, *Phys. Rev. Lett.* **126** (2021) 061604 [2011.12005].

[25] I. Akal, Y. Kusuki, N. Shiba, T. Takayanagi and Z. Wei, *Holographic moving mirrors*, *Class. Quant. Grav.* **38** (2021) 224001 [2106.11179].

[26] A. Mollabashi, N. Shiba, T. Takayanagi, K. Tamaoka and Z. Wei, *Aspects of pseudoentropy in field theories*, *Phys. Rev. Res.* **3** (2021) 033254 [2106.03118].

[27] H. Omiya and Z. Wei, *Causal structures and nonlocality in double holography*, *JHEP* **07** (2022) 128 [2107.01219].

[28] I. Akal, T. Kawamoto, S.-M. Ruan, T. Takayanagi and Z. Wei, *Page curve under final state projection*, *Phys. Rev. D* **105** (2022) 126026 [2112.08433].

[29] I. Akal, T. Kawamoto, S.-M. Ruan, T. Takayanagi and Z. Wei, *Zoo of holographic moving mirrors*, *JHEP* **08** (2022) 296 [2205.02663].

[30] P. C. W. Davies and S. A. Fulling, *Radiation from a moving mirror in two-dimensional space-time conformal anomaly*, *Proc. Roy. Soc. Lond. A* **348** (1976) 393.

[31] S. Gao and R. M. Wald, *Theorems on gravitational time delay and related issues*, *Class. Quant. Grav.* **17** (2000) 4999 [gr-qc/0007021].

[32] E. Witten, *Light Rays, Singularities, and All That*, *Rev. Mod. Phys.* **92** (2020) 045004 [1901.03928].

[33] L. Randall and R. Sundrum, *A Large mass hierarchy from a small extra dimension*, *Phys. Rev. Lett.* **83** (1999) 3370 [hep-ph/9905221].

[34] L. Randall and R. Sundrum, *An Alternative to compactification*, *Phys. Rev. Lett.* **83** (1999) 4690 [hep-th/9906064].

[35] P. Francesco, P. Mathieu and D. Sénéchal, *Conformal field theory*. Springer Science & Business Media, 1997.

[36] A. Karch and L. Randall, *Open and closed string interpretation of SUSY CFT's on branes with boundaries*, *JHEP* **06** (2001) 063 [hep-th/0105132].

[37] R. Bousso and L. Randall, *Holographic domains of anti-de Sitter space*, *JHEP* **04** (2002) 057 [hep-th/0112080].

[38] O. Aharony, O. DeWolfe, D. Z. Freedman and A. Karch, *Defect conformal field theory and locally localized gravity*, *JHEP* **07** (2003) 030 [hep-th/0303249].

[39] M. Porrati, *Mass and gauge invariance 4. Holography for the Karch-Randall model*, *Phys. Rev. D* **65** (2002) 044015 [hep-th/0109017].

[40] D. Neuenfeld, *The Dictionary for Double-Holography and Graviton Masses in d Dimensions*, 2104.02801.

[41] H. Geng and A. Karch, *Massive islands*, *JHEP* **09** (2020) 121 [2006.02438].

[42] M. A. Nielsen and I. L. Chuang, *Quantum Computation and Quantum Information*. Cambridge University Press, 2000.

[43] M. J. Donald, M. Horodecki and O. Rudolph, *The uniqueness theorem for entanglement measures*, *Journal of Mathematical Physics* **43** (2002) 4252–4272 [quant-ph/0105017].

[44] M. Srednicki, *Chaos and quantum thermalization*, *Phys. Rev. E* **50** (1994) 888 [cond-mat/9403051].

[45] P. Calabrese and J. Cardy, *Entanglement entropy and quantum field theory*, *Journal of Statistical Mechanics: Theory and Experiment* **2004** (2004) P06002.

[46] P. Calabrese and J. Cardy, *Entanglement entropy and conformal field theory*, *Journal of Physics A: Mathematical and Theoretical* **42** (2009) 504005.

[47] A. Lewkowycz and J. Maldacena, *Generalized gravitational entropy*, *JHEP* **08** (2013) 090 [1304.4926].

[48] V. E. Hubeny, M. Rangamani and T. Takayanagi, *A Covariant holographic entanglement entropy proposal*, *JHEP* **07** (2007) 062 [0705.0016].

[49] T. Faulkner, A. Lewkowycz and J. Maldacena, *Quantum corrections to holographic entanglement entropy*, *JHEP* **11** (2013) 074 [1307.2892].

[50] N. Engelhardt and A. C. Wall, *Quantum Extremal Surfaces: Holographic Entanglement Entropy beyond the Classical Regime*, *JHEP* **01** (2015) 073 [1408.3203].

[51] Y. Kusuki and Z. Wei, *AdS/BCFT from conformal bootstrap: construction of gravity with branes and particles*, *JHEP* **01** (2023) 108 [2210.03107].

[52] J. Sully, M. Van Raamsdonk and D. Wakeham, *BCFT entanglement entropy at large central charge and the black hole interior*, *JHEP* **03** (2021) 167 [2004.13088].

[53] S. S. Gubser, I. R. Klebanov and A. M. Polyakov, *Gauge theory correlators from noncritical string theory*, *Phys. Lett.* **B428** (1998) 105 [hep-th/9802109].

[54] E. Witten, *Anti-de Sitter space and holography*, *Adv. Theor. Math. Phys.* **2** (1998) 253 [hep-th/9802150].

[55] H. Casini, M. Huerta and R. C. Myers, *Towards a derivation of holographic entanglement entropy*, *JHEP* **05** (2011) 036 [1102.0440].

[56] H. Geng, A. Karch, C. Perez-Pardavila, S. Raju, L. Randall, M. Riojas et al., *Information Transfer with a Gravitating Bath*, *SciPost Phys.* **10** (2021) 103 [2012.04671].

[57] R.-X. Miao, *An Exact Construction of Codimension two Holography*, *JHEP* **01** (2021) 150 [2009.06263].

[58] R.-X. Miao, *Codimension-n holography for cones*, *Phys. Rev. D* **104** (2021) 086031 [2101.10031].

[59] N. Ogawa, T. Takayanagi, T. Tsuda and T. Waki, *Wedge Holography in Flat Space and Celestial Holography*, 2207.06735.

[60] S. W. Hawking and G. F. R. Ellis, *The large scale structure of space-time*, vol. 1. Cambridge university press, 1973.

[61] J. Cardy, *The $T\overline{T}$ deformation of quantum field theory as random geometry*, *JHEP* **10** (2018) 186 [1801.06895].

[62] F. Piazza and A. J. Tolley, *Subadditive Average Distances and Quantum Promptness*, 2212.06156.

[63] A. B. Zamolodchikov, *Expectation value of composite field T anti-T in two-dimensional quantum field theory*, hep-th/0401146.

[64] F. A. Smirnov and A. B. Zamolodchikov, *On space of integrable quantum field theories*, *Nucl. Phys. B* **915** (2017) 363 [1608.05499].

[65] L. McGough, M. Mezei and H. Verlinde, *Moving the CFT into the bulk with $T\overline{T}$*, *JHEP* **04** (2018) 010 [1611.03470].

[66] A. Lewkowycz, J. Liu, E. Silverstein and G. Torroba, *$T\overline{T}$ and EE, with implications for (A)dS subregion encodings*, *JHEP* **04** (2020) 152 [1909.13808].

[67] B. Grado-White, D. Marolf and S. J. Weinberg, *Radial Cutoffs and Holographic Entanglement*, *JHEP* **01** (2021) 009 [2008.07022].

[68] H. Ishihara, *Causality of the brane universe*, *Phys. Rev. Lett.* **86** (2001) 381 [gr-qc/0007070].

[69] Y. Aharonov, D. Z. Albert and L. Vaidman, *How the result of a measurement of a component of the spin of a spin-1/2 particle can turn out to be 100*, *Physical review letters* **60** (1988) 1351.

[70] S. Sachdev, *Quantum phase transitions*, *Physics world* **12** (1999) 33.

[71] P. Weinberg and M. Bukov, *QuSpin: a python package for dynamics and exact diagonalisation of quantum many body systems part i: spin chains*, *SciPost Physics* **2** (2017) .

[72] A. Karch and L. Randall, *Geometries with mismatched branes*, *JHEP* **09** (2020) 166 [2006.10061].

[73] S. Cooper, M. Rozali, B. Swingle, M. Van Raamsdonk, C. Waddell and D. Wakeham, *Black hole microstate cosmology*, *JHEP* **07** (2019) 065 [1810.10601].

[74] H. Geng, S. Lüst, R. K. Mishra and D. Wakeham, *Holographic BCFTs and Communicating Black Holes*, 2104.07039.

[75] S. B. Giddings, *The deepest problem: some perspectives on quantum gravity*, 2202.08292.

[76] A. Karch, H. Sun and C. F. Uhlemann, *Double holography in string theory*, *JHEP* **10** (2022) 012 [2206.11292].

[77] R. Emparan, A. M. Frassino and B. Way, *Quantum BTZ black hole*, *JHEP* **11** (2020) 137 [2007.15999].

[78] P. Bueno, R. Emparan and Q. Llorens, *Higher-curvature gravities from braneworlds and the holographic c-theorem*, *Phys. Rev. D* **106** (2022) 044012 [2204.13421].

[79] R. Emparan, J. F. Pedraza, A. Svesko, M. Tomašević and M. R. Visser, *Black holes in dS_3*, *JHEP* **11** (2022) 073 [2207.03302].

[80] Y. Li, X. Chen and M. P. A. Fisher, *Quantum Zeno effect and the many-body entanglement transition*, *Phys. Rev. B* **98** (2018) 205136 [1808.06134].

[81] B. Skinner, J. Ruhman and A. Nahum, *Measurement-Induced Phase Transitions in the Dynamics of Entanglement*, *Phys. Rev. X* **9** (2019) 031009 [1808.05953].

[82] Y. Li, X. Chen and M. P. A. Fisher, *Measurement-driven entanglement transition in hybrid quantum circuits*, *Phys. Rev. B* **100** (2019) 134306 [1901.08092].